Palaeogeography, Palaeoclimatology, Palaeoecology 285 (2010) 205–223

Contents lists available at ScienceDirect

Palaeogeography, Palaeoclimatology, Palaeoecology

journal homepage: www.elsevier.com/locate/palaeo

Lead isotopic evidence for an Australian source of aeolian dust to Antarctica at times over the last 170,000 years

Patrick De Deckker [a,*], Marc Norman [a], Ian D. Goodwin [b], Alan Wain [c], Franz X. Gingele [d]

[a] Research School of Earth Sciences, The Australian National University, Canberra ACT 0200, Australia
[b] Climate Risk CoRE, Department of Environment and Geography, Macquarie University NSW 2109, Australia
[c] CAWCR — High Impact Weather Team, Bureau of Meteorology, PO Box 1636, Melbourne VIC 3001, Australia
[d] Formerly of Department of Earth and Marine Sciences, The Australian National University, Canberra ACT 0200, Australia

ARTICLE INFO

Article history:
Received 29 March 2009
Received in revised form 28 October 2009
Accepted 12 November 2009
Available online 20 November 2009

Keywords:
Pb
Sr
Nd isotopes
Murray Darling Basin
Airborne dust
EPICA
Vostok
Antarctic ice cores
Patagonia
Argentina

ABSTRACT

Systematic analysis of Pb, Sr and Nd isotopes of 32 fluvial clay samples (<2 μm fraction) from many of the major tributaries of the vast (1.10^6 km^2) Murray Darling Basin (MDB), located in semiarid southeastern Australia, displays similar isotopic values between some MDB clays and dust from several ice core samples from the EPICA Dome C in Antarctica. Close scrutiny of several ratios of the four Pb isotopes, and in particular $^{208}Pb/^{207}Pb$ versus $^{206}Pb/^{207}Pb$, shows that several samples from the Darling-sub-basin of the MDB display similar values for the same isotopes for Dome C samples from different ages, and more particularly during wet phases in Australia [Marine Isotopic Stages 5e, 3 and 1]. The combination of Nd and Sr isotopic ratios from the same MDB fluvial clays clearly eliminates the Murray sub-basin, and supports the Darling sub-basin as a potential source of aeolian material to Antarctica. Overall, the Australian dust supply to Antarctica predominantly occurred during interglacial periods.

The work presented here shows that aerosols generated in southeastern Australia can travel to parts of West Antarctica and this is supported by atmospheric observations and models. In addition, evidence of Australian dust in Antarctic ice cores further implies dust deposition in the Southern Ocean would have occurred in the past. Current meteorological observations also imply that the western Pacific and Indian Ocean sector of the Southern Ocean would frequently receive aeolian dust components originating from southeastern Australia.

1. Introduction

After Antarctica, Australia is the driest continent. There is ample evidence that during the Last Glacial Maximum (LGM), in particular, the central Australian desert zone expanded towards the coast (Bowler, 1976). This also would have been the case during previous dry phases that coincided with Marine Isotopic Stages (MIS) such as MIS 4, 6, 8 and 10 when major lakes in Australia would have dried up and dune fields were active. On land, an extremely wet period that commenced around 60 ka coincided with what is called the "mega-lake" phase when many lakes were permanently filled, and that was synchronous with MIS 3 (Bowler et al., 2006). However, by approximately 35 ka, lake levels started to drop and the world entered into the very cold and dry phase [especially Australia; see Miller et al. (1997) and Barrows et al. (2000)] that culminated at the LGM. During the latter period, dune mobility was extensive throughout Australia and airborne dust would have spread across the continent and into the surrounding oceans and adjacent landmasses.

Jennings (1968) determined that the major direction of the winds in Australia follows an anticlockwise gyre (Jennings, 1968) with two major plumes of aeolian material spreading over the Tasman Sea in the southeast and the eastern Indian Ocean in the northwest (Bowler, 1976). More recently, Sturman and Tapper (2006) have reassessed the characteristic late winter (August) atmospheric transport patterns in the Australasian region and have identified a more complex set of major, near-surface airflow directions for a larger number of locations that pass over the margin of the Australian continent compared to what was previously identified (Fig. 1). Previous studies (Grousset et al., 1992; Basile et al., 1997; Delmonte et al., 2004, 2007, 2008; Gaiero, 2007) concluded that dust transported to Antarctica (during the LGM) was sourced from South America and primarily from Patagonia, and that dust export from Australia could be excluded. An exception is the recent study of Revel-Rolland et al. (2006), which pointed out that Lake Eyre in central Australia may have contributed to dust deposited at Dome C. A second paper by Marino et al. (2008), based on major elemental composition of aeolian dust recovered from Dome C, concluded that Australia was a possible source of dust during warm phases, notably the Holocene.

It is clear that there is a need to establish the origin of aeolian dust deposited in Antarctica. Has dust always come from the same source or have sources varied through time? Have different sources supplied

* Corresponding author.
E-mail address: patrick.dedeckker@anu.edu.au (P. De Deckker).

0031-0182/$ – see front matter © 2009 Elsevier B.V. All rights reserved.
doi:10.1016/j.palaeo.2009.11.013

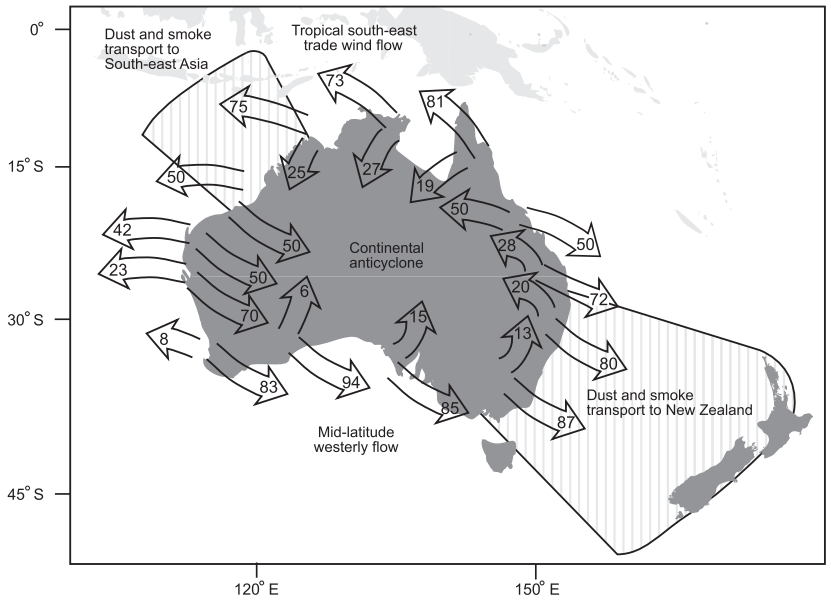

Fig. 1. Map of Australia showing characteristic late winter (August) atmospheric transport patterns in the Australasian region calculated from atmospheric trajectories. Block arrows represent the major near-surface airflow directions and percent occurrence for a number of locations on the margin of the Australian continent. Note the large amount of anticyclonic and offshore transport, even on the coast of Queensland, along the northeast coast of Australia. [Reproduced by permission of Oxford University Press Australia from Sturman and Tapper (2006; Fig. 3.21)].

dust simultaneously? These are important questions because, by determining dust sources, it will become possible to reconstruct atmospheric circulation at high latitudes in the Southern Hemisphere through time, especially over significant periods of climate change.

This paper is an attempt to evaluate those questions based on isotopic evidence obtained from an array of fluvial samples from the extensive Murray Darling Basin of southeastern Australia (Figs. 2 and 3). In addition, the recent access to satellite imageries and meteorological

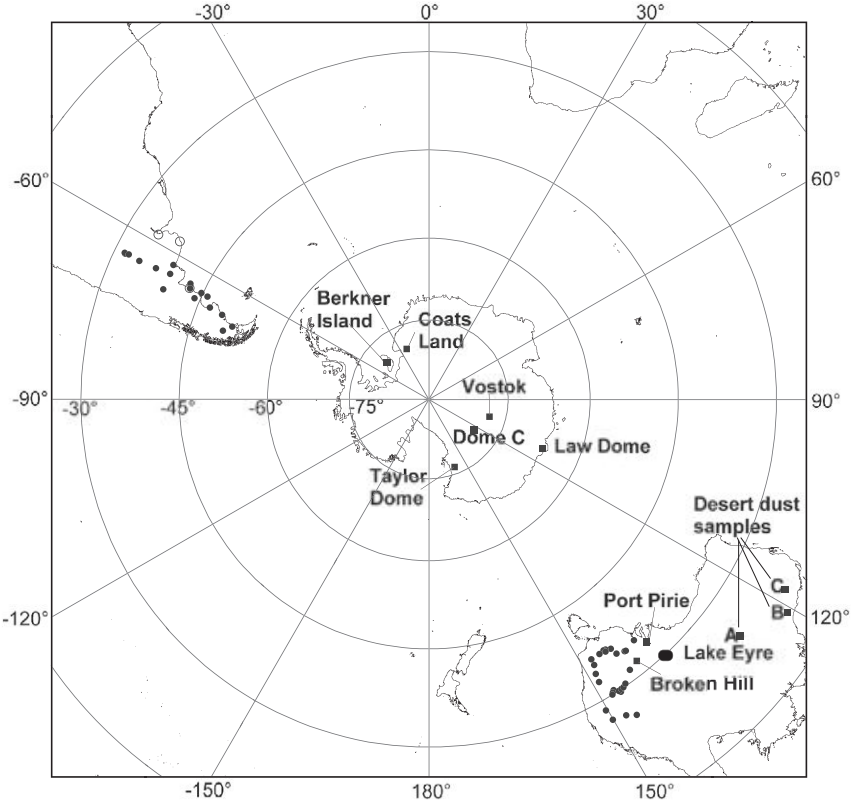

Fig. 2. Map showing the location of all the sites mentioned in the text. For South America, open circles are data from Delmonte et al. (2004), and from B. Delmonte (pers. com. to De Deckker). Black circles are data of Gaiero (2007). The fluvial samples in the MDB are those analysed by Gingele and De Deckker (2005). Note that for the Australian MDB, 23 samples were analysed for Pb isotopes and 26 for Sr and Nd isotopes. The location of 3 desert dust samples taken from the Great Sandy Desert in Western Australia which lie above Archean rocks is also shown. Sample A is from the Central Desert, B and C from the Great Sandy Desert; these samples are the same as those mentioned in Gingele et al. (2007) and De Deckker et al. (2008).

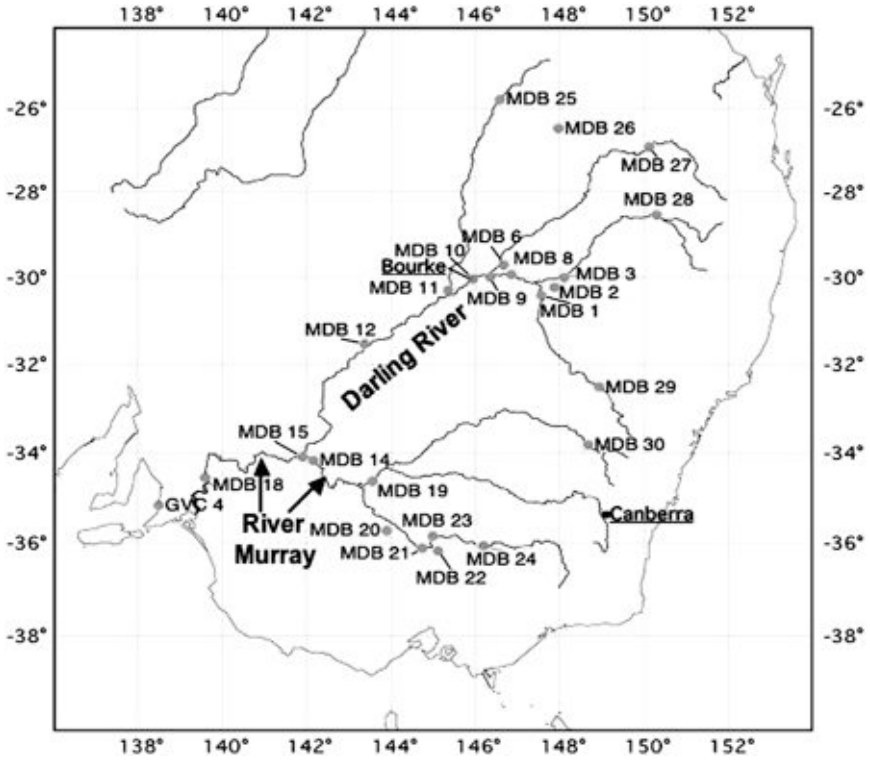

Fig. 3. Map showing the location of all the fluvial samples obtained from the Murray Darling Basin. The samples are the same as those studied by Gingele and De Deckker (2005) and for which Sr and Nd isotopic analyses have already been published. Note that sample MDB15 is located at the junction of the 2 main rivers (Darling and Murray) which each have several important tributaries.

reanalysis data and back/forward trajectory modelling show that, in fact, air masses–some of which carry airborne dust–leave Australia in any possible direction depending on meteorological conditions at the time. It is now clear that some air masses do circumnavigate Antarctica and, therefore, there is potential for Australian dust to reach Patagonia and even the Antarctic mainland (see section below and Fig. 4).

2. Atmospheric circulation over the Southern Ocean and Antarctica

Over the Antarctic continent, low level winds are dominated by downslope katabatic flows from the elevated interior towards the coast. Topography is also important in determining the final strength of the wind; some areas of confluence result in very high wind speeds. The low level flow at the continental margin is generally anticyclonic, a result of Coriolis forces, and the meridional circulation. At levels above 500 hPa, the situation is reversed and a generally cyclonic circulation exists with subsidence over the centre of the continent and flows directed towards the pole (King and Turner, 1997).

Moving north from the Antarctic coast, one of the large-scale features of southern hemisphere weather is the band of semi-permanent, low pressure extending around the Antarctic continent, known as the circumpolar trough. Located along the boundary where continental air meets warmer maritime air, this region is also a dividing line between low-level westerly (to the north) and easterly (to the south) wind regimes. The average position of the deepest part of the circumpolar trough is around latitude 66°S, although it expands and contracts equatorward/poleward as a result of atmospheric mass exchanges with the mid-latitudes on semi-annual to multi-decadal timescales (Sinclair et al., 1997; Simmonds and Keay, 2000).

The zone of strongest winds (50–45°S), located just northward of the Antarctic Circumpolar Ocean Current (ACC), appears to have moved south in recent decades, as part of the shift towards the high (positive) phase of the Southern Annular Mode (SAM), thus increasing the strength of the ACC. The SAM is the dominant climate mode in the Southern Hemisphere (Sinclair et al., 1997), and represents the zonal (poleward–equatorward) vacillation in pressure and winds between the mid-latitudes (40 to 45°S) and the high latitudes (65°S), and is coupled to the behaviour of the subtropical anticyclone over Australia (Rogers and van Loon, 1982). Toggweiler and Russell (2008) and others such as Thompson and Solomon (2002) have attributed the recent poleward migration of the SAM and an accompanying intensification of the westerly winds to changes in the thermal contrast of the mid-level atmosphere over the last 40 years in response to increases in atmospheric O_3 and CO_2 levels. There is limited information on past variability in the SAM as a result of natural dynamics, solar, volcanic forcing and ocean circulation feedbacks. Goodwin et al. (2004) showed in their proxy sea-level pressure (SLP) record over the past 700 years, evidence for a shift from negative SAM (weaker westerlies) during the 13th and 14th centuries to positive SAM (stronger westerlies) during the 17th and 18th centuries. Positive SAM index circulation is characterized by a strengthening of the westerlies and a poleward shift in the circumpolar trough, whilst during a negative SAM index circulation a weakening of the westerlies and an equatorward shift in the circumpolar trough, drives a more meridional air flow between the southern mid-latitudes and the Antarctic continent. The past variability of the SAM is of interest, with respect to dust transport. The Toggweiler and Russell (2008) hypothesis is that the Last Glacial Maximum was not as windy as previously thought due to low CO_2 levels and a weaker mid-atmosphere thermal contrast. This is supported by the modelling results of Justino and Peltier (2006) who found a positive SAM type for the LGM. (shown in Fig. 5). This is characteristic of weakened westerlies in the high southern latitudes and an enhanced meridional transport from the mid-latitudes to Antarctica.

Whilst dust transport mechanisms are a primary driver of dust flux variability in the Southern Hemisphere atmosphere, changes in the source environments and dust entrainment may be equally important in understanding extant dust flux deposition histories. Today, many parts of

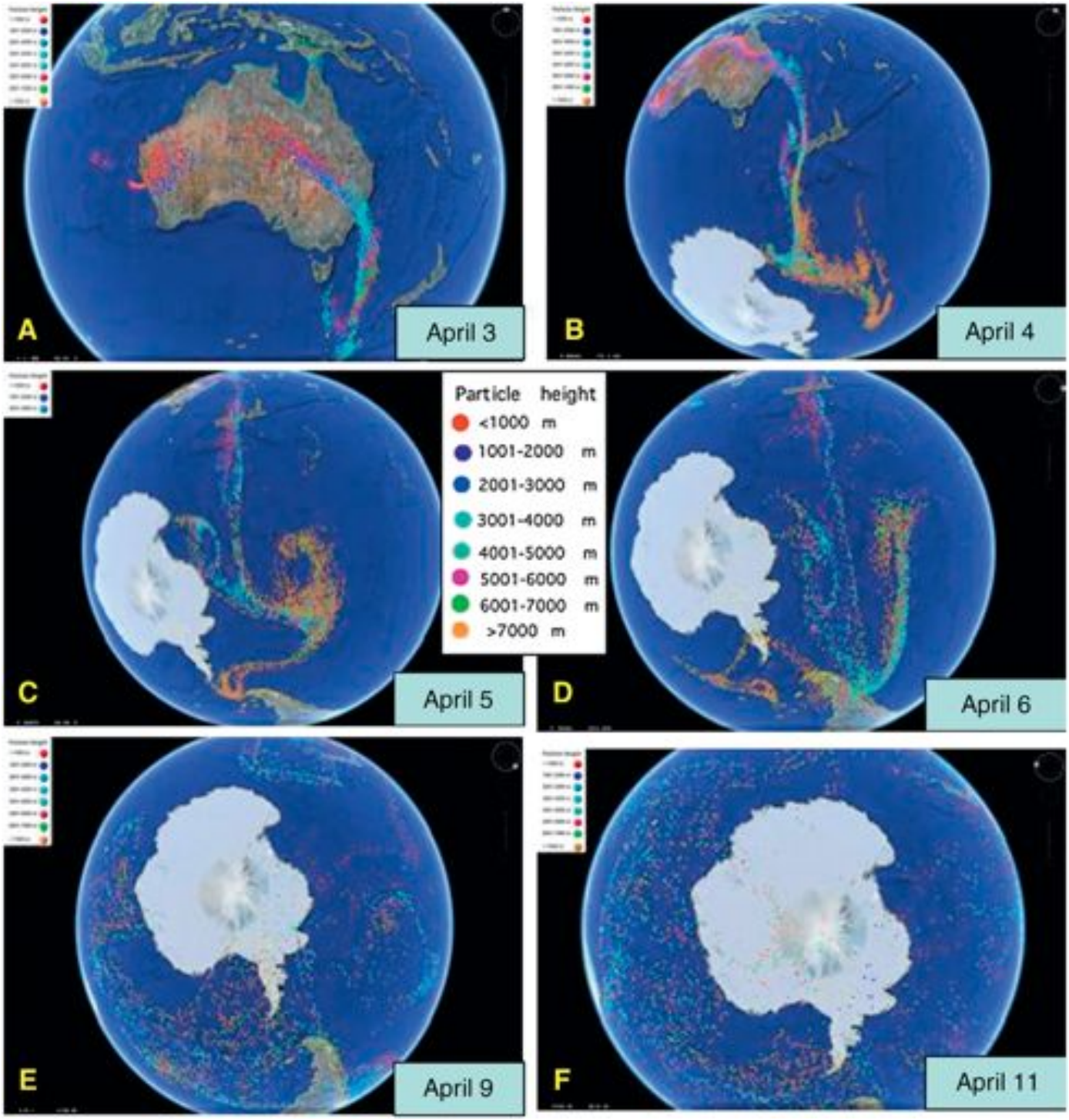

Fig. 4. Composite set of maps displayed on NASA satellite images (displayed with the use of Google Earth™ software) that show the simulated evolution of an airmass over a period of 11 days commencing on April 1, 2008 when a major dust storm passed through many towns in southeastern Australia that had devastating effects on many buildings in Tasmania. Time of images is 0000 UTC in all cases. Note that the air masses completely circumnavigate Antarctica and that, in particular, the particles travelled over the Ross Sea (B–C), the tip of Patagonia (C–E) and the Weddell Sea (E–F). Coloured circles along the calculated trajectories show different heights [insert] of the modelled particles.

southern Australia are becoming increasingly dry. This arid phase commenced about 6 Ka coinciding with a progressive drop in sea-surface temperature (Calvo et al., 2007), increased prominence of the El Nino Southern Oscillation (Gagan et al., 2000; Moros et al., 2009), frequent lake level fluctuations (Bowler, 1981; De Deckker, 1982) and changed wind intensities (see Stanley and De Deckker, 2002). As a consequence, Australia is experiencing periods of severe droughts during which dust deflation and dust storms have become more common, with one of the best modern examples occurring around October 22–23, 2002 which received much scientific attention (McTainsh et al., 2005; Chan et al., 2005; Wain et al., 2006; De Deckker et al., 2008).

3. Provenance of dust in Antarctica

Until recently, the concept that Patagonia is the major source of dust in Antarctic ice cores has become entrenched in the literature, based

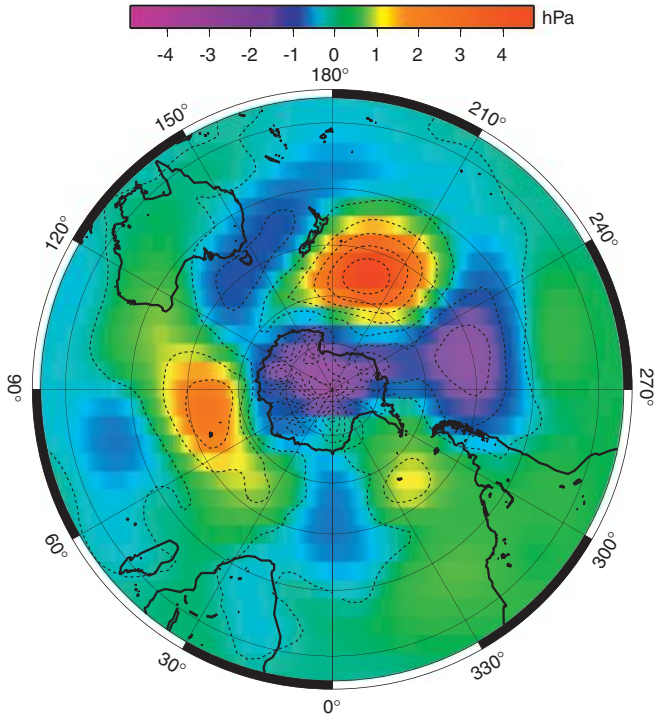

Fig. 5. Plot of the hemispheric 500 hPa geopotential height anomalies associated with the primary atmospheric circulation mode in the GCM model output for LGM winter by Justino and Peltier (2006). They calculated these from the model output by regressing the model geopotential height anomalies upon the leading empirical orthogonal function (EOF) for the Southern Hemisphere pressure field. This figure describes the extratropical pressure pattern (wave train) associated with the propagation of tropical Pacific anomalies into the extratropics that is associated with the ENSO climate mode. The sign of the anomalies with high pressure over the New Zealand region and low in the Amundsen Sea off West Antarctica is typical of La Nina-like years. Meridional dust transport into the Antarctic is controlled by southward meridional airflow associated with high pressure anomalies over the New Zealand region.
(Reproduced by permission of American Geophysical Union).

mostly on Sr and Nd isotopic compositions (see Basile et al., 1997; Delmonte et al., 2004, 2007, 2008; Gaiero, 2007). This concept has been backed by several modellers (viz. Lunt and Valdes, 2002) despite the fact that Joussaume (1993) had already strongly argued that Australia today is the most significant dust source in the Southern Hemisphere, arguing that the prevailing transport of dust is westward and is associated with middle latitudes. She concluded (Joussaume (1993) that *"in February, dust deposits over Antarctica mainly come from South America and Australia, whereas in August the Australian source is the prevailing one"*… and *"On annual mean, the Australian source prevails, especially over East Antarctica"*. It took 15 years to return to Joussaume's (1993) views; for example, see Li et al. (2008). Those latter authors clearly define that Australia is also a major dust supplier in the Southern Hemisphere (Australia: 120 Tg a^{-1}, Patagonia: 38 Tg a^{-1}; and the inter-hemispheric transport from the Northern Hemisphere: 31 Tg a^{-1}; for more information, refer to Li et al., 2008). In addition, Li et al. (2008) conclude their paper by saying that *"the location of Vostok station is close to the boundary of South American (45%) and Australian (35%) dominant regions for dust deposition"*.

The most convincing geochemical evidence for an Australian source of Antarctic dust is provided by the work of Vallelonga et al. (2002b) through the geochemical fingerprinting ($^{206}Pb/^{207}Pb$) of samples from an ice core of snow [obtained in a firn core] that fell at Law Dome in Antarctica (Fig. 3) near the coast of Wilkes Land. Some of the Law Dome samples have a Pb isotopic composition in a specific interval that is characteristic of the Australian Broken Hill lead mine (Fig. 3), which Vallelonga et al. (2002b) suggest would have originated from smelters either at the mine itself or from another site smelting Broken Hill ore near the coast at Port Pirie in South Australia (Fig. 3). Vallelonga et al. (2002b) identified that, for the time interval spanning 1884 to 1908 AD, a four-fold increase in Pb concentration was associated with a shift in Pb isotopic compositions to $^{206}Pb/^{207}Pb$ ratios identical to the ore at Broken Hill, and were distinct from other sources such as Ross Island basanitoids, pelagic sediments in the Southern Hemisphere and South Sandwich Island sediments. This demonstrates that air masses can travel across the Southern Ocean between Australia and Antarctica transporting Pb aerosols that were mixed in snow that eventually became ice and firn.

Joussaume (1993) argued for Australia as a dust source to Antarctica during the LGM and for a *"poleward displacement of the low located south of Australia"*. Nevertheless, she concluded that her model required further verification as *"no kaolinite had been observed in the microparticle analyses of dust deposits of Dome C and Vostok for the LGM as reported by Gaudichet et al. (1988)"*. It is unfortunate that knowledge of Australian surficial clay mineralogy was poorly documented at the time, as the more recent work of Gingele and De Deckker (2005) clearly documents a wide spectrum of mineralogies, including kaolinite, for potential Australian sources of dust, including the Murray Darling Basin (MDB) sediments of interest here. Already, Revel-Rolland et al. (2006) have pointed to parts of Australia being a possible source of aeolian dust to Antarctica by fingerprinting different Australian sources to Antarctica based on Nd and Sr isotopic ratios. Based on additional fluvial samples collected from the vast MDB, we seek to test the hypothesis of Revel-Rolland and colleagues, by presenting new Pb isotopic data, as well as previously published Nd and Sr isotopic analyses carried out on the same samples.

4. Climatology of the 1884 to 1908 period, a long period of drought in Australia

The Law Dome ice core samples with Pb isotopic compositions characteristic of Broken Hill were deposited at a time when the most extreme negative Southern Oscillation Index (SOI) values for the past century of −42.2 and −42.6 occurred in 1896 and 1905. This coincided with severe El Nino events that resulted in the prolonged extreme drought conditions over southern Australia, and hence, enhanced occurrence of dust raising. Whilst instrumental observations of the atmospheric circulation are sparse for this time, the proxy circulation interpretations of Goodwin et al. (2004) provide some insight. These authors reconstructed the monthly Southern Ocean sea level pressure (SLP) anomalies over the past 700 years from sea-salt sodium (Na) concentrations in the Law Dome (DSS) ice core calibrated to sea-level pressure and wind field variability over the Southern Ocean and Australian mid-latitudes. They established through calibrations to the instrumental SLP records and the Southern Annular Mode (SAM) Index that the proxy record robustly describes the early winter variability in the SAM, in the south Indian to southwest Pacific longitudes. Low Na (High Na) concentrations at DSS occur during positive (negative) SAM circulation where the westerlies and the associated transient low-pressure systems track equatorward (poleward), with an enhanced north–south (westerly) meridional (zonal) air transport (Goodwin et al., 2004). The characteristic SLP anomalies associated with low Na concentrations in the DSS ice core are shown in Fig. 6.

During the 1884 to 1908 period, the low DSS Na concentrations indicate that high mid-latitude winter SLP anomalies occurred over southern Australia, and that the circulation pattern had shifted to the most positive SAM index phase, with a poleward displacement of the Subtropical Anticyclone and strengthened westerlies in Antarctic latitudes. Typically, under a positive SAM circulation, high pressure anomalies occur south of the Tasman Sea and south-east of New Zealand and are associated with a high frequency of winter atmospheric blocking (Renwick and Revell, 1999; Sinclair et al., 1997) that can cause ridging into East Antarctica (Goodwin et al., 2003). This pattern produces ridging and a northerly wind anomaly

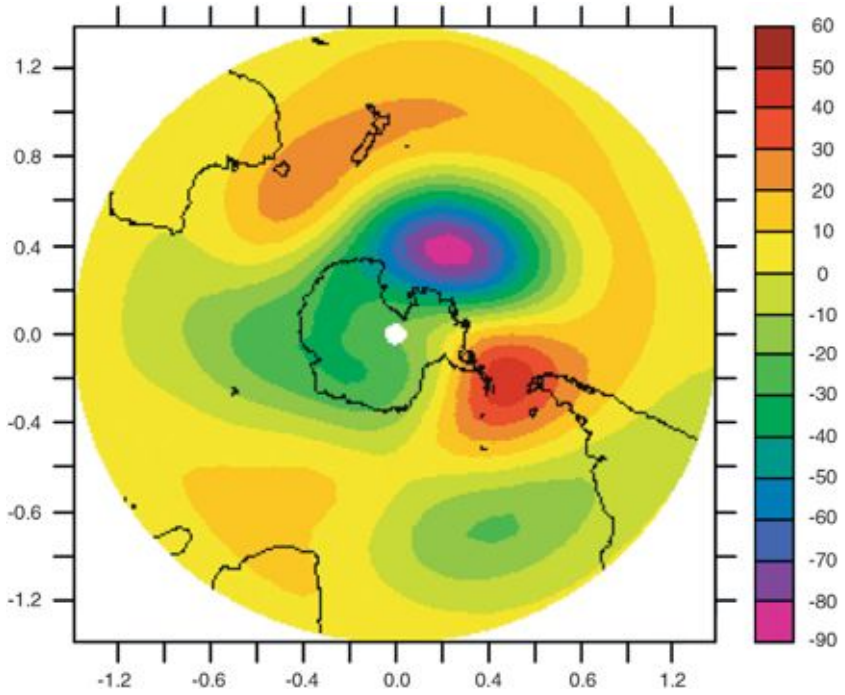

Fig. 6. The spatial pattern of early winter sea-level pressure anomalies (NCEP–NCAR Reanalysis) for years with low sea-salt Na concentration in the Law Dome (DSS) ice core from East Antarctica. This pattern is representative of the circulation anomalies associated with a positive SAM (low pressure anomaly over Antarctica) and (high pressure anomaly to the south-east of Australia and New Zealand) described by the Pacific South American (PSA) as mode 1 negative (La Nina phase of ENSO) in the extratropics, after Goodwin et al. (2004).

across the circumpolar trough south of south-eastern Australia (Goodwin et al., 2004: Fig. 5b) and produces a direct air trajectory across the Southern Ocean for aerosol transport from the Broken Hill region located on the edge of the Murray Darling Basin, along the poleward limb of the subtropical anticyclone.

5. Murray–Darling Basin

The Murray Darling Basin (MDB) covers 1,073,000 km^2 of southeast Australia and drains 14% of the Australian landmass. The Basin extends over 2 climatic zones, being influenced by the tropical monsoon in the North and the westerlies in the South, resulting in highly variable and episodic river discharge and sediment transport. The Murray and Darling Rivers and their tributaries travel through a variety of geological formations, each of which have their peculiarities and specific geochemical and mineralogical compositions (Gingele and De Deckker, 2005). Erosion and weathering of the unique combination of rock formations within each catchment imprint characteristic mineralogical, elemental, and isotopic signatures onto the sediments transported downriver. The northern tributaries of the Darling River originate in Mesozoic clastic sediments of South Central Queensland while the eastern tributaries drain the western slopes of the Great Dividing Range. Rock formations in that area consist of widespread Tertiary volcanics, Mesozoic granites and late Palaeozoic volcanics, metasediments and granites, in the southern part of the New England Foldbelt (Rutland, 1976). South of this, the Lachlan Foldbelt includes early Palaeozoic granites, volcanics and metasediments. Similar rock formations continue into the Southern Highlands. Incidentally, all the Murray tributaries originate in the Lachlan Foldbelt or the Southern Highlands, while the Darling tributaries, except for the Macquarie River, drain the New England Foldbelt and South Central Queensland. The different composition and age of these major geological units weather to characteristic and different soils in both catchments (Butler and Hubble, 1978). The suspended loads of the tributaries in the MDB should contain characteristic signatures derived from the parent rocks and soils in the respective catchments.

Today, the Murray–Darling fluvial system is heavily managed and water flow has diminished to one-third of the natural flow near Murray Bridge (Close, 1990). The sediment transported today is mainly suspended clays. The isotopic and geochemical signatures of suspended matter in the Murray–Darling fluvial system also depend on the size fraction (Douglas et al., 1995). Because a large part of the suspended matter in the Murray–Darling fluvial system consists of the clay fraction and to keep data from all tributaries comparable, we used the fraction <2 μm for all our fingerprinting analyses. The analysis of the clay fraction from the MDB also permits comparison with the isotopic composition of dust from Antarctic ice cores, which is also <2 μm.

6. Material and methods

6.1. Fluvial clays

The Murray and Darling rivers and their tributaries and anabranches were sampled at 26 locations throughout the basin (Figs. 2 and 3). Emphasis was laid on obtaining clayey material. Preferred sampling sites were deposits of suspended matter from previous flooding events, such as dried-out mudpools in river beds and bank sediments, which contain a sequence of previous flooding events. Such samples should therefore yield an average composition of the fine-grained fraction of the regolith within the entire catchment of a particular river/tributary. The samples are not representative of the grain size or bulk mineralogical composition of the material transported in the rivers. However, we believe that they represent the clay mineral suite of the fraction <2 μm, which is transported in suspension.

For clay mineral analysis, samples were first washed through a 63 μm mesh sieve. The fines were retained in a 10 l container, decanted, and then treated with hydrogen peroxide (10%) and acetic acid (10%) at room temperature, to remove organic matter and carbonate respectively and to disaggregate the particles. Subsequently, the samples were split into silt (2–63 μm) and clay (<2 μm) fractions by conventional settling techniques.

6.2. Pb isotopes

Pb isotopic analyses were carried out at the Research School of Earth Sciences, Australian National University. The powdered samples were dissolved in HF–HNO_3 in screw-cap Teflon vials. Sr and Nd isotopic analyses, carried out on the same samples, were presented in Gingele and De Deckker (2005). Pb was isolated using anion exchange chromatography (Chen and Wasserburg, 1981). The sample was loaded on the column in dilute (0.8 N) HBr and the Pb was eluted with 6 N HCl. The eluted Pb from each sample was dried, dissolved in 2 ml of 2% HNO_3 and spiked with a thallium isotopic standard (NIST SRM-997) for mass bias corrections by normalisation to the NIST certified value of $^{203}Tl/^{205}Tl = 2.387$. (White et al., 2000). Pb isotopic compositions were measured on a ThermoFinnigan Neptune multi-collector magnetic-sector ICPMS operated in static mode. Each analysis consisted of 15 cycles of 8 s integrations. For the samples analysed in this study, we obtained ^{204}Pb signals of ~20–900 mV, corresponding to 2 σ measurement errors of ±0.2 to ±0.02% on $^{206}Pb/^{204}Pb$, $^{207}Pb/^{204}Pb$, and $^{208}Pb/^{204}Pb$. For a more precise comparison with the ice core data, we also present these data as $^{206}Pb/^{207}Pb$ and $^{208}Pb/^{207}Pb$ ratios, which have 2 σ measurement errors of ±0.005–0.018%. Replicate analyses of the NIST SRM-981 Pb isotopic reference material run with these samples gave the following values; uncertainties are 2 σ ($n = 7$) and comparison values in parentheses are from Woodhead et al. (1995) measured by double spike TIMS: $^{206}Pb/^{204}Pb = 16.931 \pm 0.005$ (16.936), $^{207}Pb/^{204}Pb = 15.484 \pm 0.004$ (15.489), $^{208}Pb/^{204}Pb = 36.680 \pm 0.007$ (36.701), $^{206}Pb/^{207}Pb = 1.09341 \pm 0.00007$ (1.09342), and $^{208}Pb/^{206}Pb = 2.1665 \pm 0.0003$ (2.1670). The 2SD reproducibility of these replicate analyses is ±0.02–0.03% for the 204-normalised ratios, ±0.007% for $^{206}Pb/^{207}Pb$, and ±0.016% for $^{208}Pb/^{206}Pb$. For comparison with the Antarctica data, the 2SD errors obtained from replicate analyses of the NIST-981 reference solution were applied to the unknowns. The Pb isotope data for the samples from the Murray Darling Basin fluvial system are presented in Table 1. Data of the same fluvial samples for Sr and Nd isotopes are already available in Gingele and De Deckker (2005).

6.3. Atmospheric dispersion model (HYSPLIT)

The dispersion model used in this study was version 4.8 of the HYbrid Single Particle Lagrangian Integrated Trajectory (HYSPLIT) model (Draxler and Hess, 1998). HYSPLIT uses a hybrid approach to model aerosol transport, with a Lagrangian framework to track the aerosol particles and an Eulerian type fixed grid to determine the concentration calculations. The initial model setup was as described by Draxler et al. (2001). Dust (PM10 particles) was emitted from potential dust source locations when the surface wind velocity caused a specified threshold friction velocity, based on the surface roughness of Kuwait desert sands, to be exceeded. In a previous study using HYSPLIT to simulate an Australian dust event, Wain et al. (2006) determined 10 m s^{-1} to be a representative value for threshold velocity and this value was adopted here.

HYSPLIT requires wind, temperature, and moisture data from a numerical weather prediction model as input. In this case, archived analysis datasets from the Australian Bureau of Meteorology's Global Analysis and Prediction System were used. At the time of the 2002 events modeled, GASP had 29 vertical levels and a horizontal resolution of approximately 83 km (T239) (BOM NMOC Operational Bulletin #52). However, the archived GASP data for the 2002 cases was degraded to a temporal resolution of 12 h and a grid point interval of 2.5° (~250 km). The temporal resolution of the archived data used for 2005 cases is 6 h, the grid spacing remaining at 2.5°. GASP has subsequently been upgraded and for 2008 cases the data have 61 vertical levels with a horizontal resolution of 0.75°. Temporal resolution remains at 6 h.

Draxler et al. (2001) confined their source locations to areas classified as desert land use. In Australia, large areas of dry lakes, ephemeral stream beds and marginal farming land may also make significant contributions to dust loading. To include these areas as possible dust sources, a 1° grid was placed over areas identified by McTainsh et al. (1989) as having an annual dust storm frequency of more than 2. The resulting grid of sites favourable to dust generation contains 194 potential dust sources. In the model runs, dust was emitted up to a maximum rate of 1 mg $m^{-2} s^{-1}$ when the surface wind speed, obtained from GASP data, exceeded 10 m s^{-1}.

7. Results

7.1. Pb isotopes

Pb isotopic compositions provide a time-integrated record of U, Th, and Pb relative abundances, and are therefore useful for fingerprinting crustal terranes and the provenance of marine and terrestrial

Table 1
Pb isotope data for fluvial sediments from the Murray Darling Basin of SE Australia.

Sample no.	River name	River system M = Murray D = Darling	$^{206}Pb/^{204}Pb$	2σ	$^{207}Pb/^{204}Pb$	2σ	$^{208}Pb/^{204}Pb$	2σ	$^{206}Pb/^{207}Pb$	2σ	$^{208}Pb/^{207}Pb$	2σ
MDB-1	Macquarie	M	18.349	0.001	15.604	0.001	38.392	0.004	1.175956	0.000035	2.460491	0.000068
MDB-2	Castlereagh	D	18.544	0.002	15.634	0.002	38.607	0.004	1.186129	0.000037	2.469404	0.000075
MDB-3	Namoi	D	18.699	0.004	15.637	0.004	38.729	0.008	1.195823	0.000043	2.476781	0.000081
MDB-6	Birrie	D	18.079	0.001	15.569	0.001	38.011	0.003	1.161253	0.000020	2.441518	0.000056
MDB-8	Barwon	D	18.592	0.003	15.639	0.002	38.644	0.005	1.188833	0.000051	2.470964	0.000072
MDB-9	Bogan	M	18.444	0.003	15.610	0.002	38.472	0.003	1.181522	0.000089	2.464545	0.000213
MDB-10	Darling	D	18.416	0.003	15.599	0.002	38.384	0.003	1.180626	0.000058	2.460751	0.000147
MDB-11	Warrego	D	18.724	0.003	15.627	0.002	38.739	0.003	1.198177	0.000081	2.478958	0.000174
MDB-12	Darling	D	18.588	0.002	15.618	0.001	38.594	0.003	1.190172	0.000046	2.471081	0.000122
MDB-14	Murray	M	17.767	0.001	15.563	0.001	37.679	0.003	1.141602	0.000060	2.421000	0.000129
MDB-15	Darling	D	17.932	0.004	15.562	0.003	37.845	0.007	1.152296	0.000090	2.431893	0.000245
MDB-18	Murray	M	18.397	0.008	15.610	0.006	38.397	0.017	1.178572	0.000083	2.459795	0.000177
MDB-19	Murrumbidgee	M	18.395	0.001	15.624	0.001	38.439	0.003	1.177335	0.000047	2.460233	0.000086
MDB-20	Loddon	M	18.548	0.002	15.638	0.002	38.645	0.003	1.186053	0.000044	2.471164	0.000138
MDB-21	Campaspe	M	17.722	0.002	15.558	0.003	37.661	0.009	1.139100	0.000072	2.420683	0.000168
MDB-22	Goulburn	M	18.497	0.002	15.624	0.002	38.473	0.005	1.183894	0.000044	2.462425	0.000134
MDB-23	Murray	M	18.610	0.003	15.639	0.004	38.560	0.010	1.189997	0.000095	2.465646	0.000139
MDB-24	Ovens	M	18.603	0.003	15.637	0.003	38.626	0.007	1.189664	0.000051	2.470127	0.000108
MDB-25	Warrego	D	18.735	0.003	15.621	0.002	38.718	0.007	1.199326	0.000044	2.478576	0.000151
MDB-26	Maranoa	D	18.323	0.002	15.594	0.002	38.181	0.006	1.175023	0.000057	2.448496	0.000121
MDB-27	Condamine	D	18.435	0.003	15.591	0.002	38.393	0.006	1.182423	0.000025	2.462575	0.000078
MDB-28	Macintyre	D	18.840	0.003	15.620	0.002	38.732	0.005	1.206139	0.000043	2.479619	0.000145
MDB-29	Macquarie	M	17.660	0.001	15.550	0.001	37.561	0.004	1.135726	0.000032	2.415505	0.000074

sediments (Chow and Patterson, 1962; Gulson, 1986; McLennan et al., 1993; Winter et al., 1997). Pb isotope signatures of aeolian dust can be used to trace regional and global patterns of atmospheric transport, and to document contributions of anthropogenic Pb in a variety of modern environments (Frank, 2002; Grousset and Biscaye, 2005). Pb isotopic compositions typically are presented as ratios of the radiogenic isotopes (masses 206, 207, 208) to the stable isotope ^{204}Pb. In applications where the total amount of Pb available for analysis is small, however (e.g. ice cores; Vallelonga et al., 2002a), limits on analytical precision can impose relatively large statistical variations on 204-normalised ratios due to the low natural abundance of this isotope (~1.4% for modern Pb). In these cases, normalisation to ^{207}Pb provides a convenient alternative as it can be considered a 'quasi-stable' isotope in modern systems due to the depletion of its parent isotope ^{235}U (half life = 704 million years) over the age of the Earth.

Examination of Fig. 7 shows that the ^{208}Pb/^{207}Pb versus ^{206}Pb/^{207}Pb plot for the MDB samples fall along a line, although there is some divergence from the overall trend. Note that error bars are quite small because relatively large samples were used, resulting on good measurement precision. On Fig. 7 also are plotted the EPICA Dome C data (Fig. 2) from Vallelonga et al. (2005), which display very large error bars due to the minute amount analysed. Samples from glacial ice intervals have smaller errors due to the increased mass available to these researchers. Numerous samples collected at Dome C plot fairly far away from the Australian overall line plot, but it is also obvious from this figure that several values from the MDB are similar, especially when error bars are taken into account. In order to compare the Australian values against other dust samples found in both ice and snow in Antarctica, we plotted Fig. 8 which shows, especially considering the error bars for the Antarctic samples, that none of the samples from Taylor Dome measured by Matsumoto and Hinkley (2001), with an age span of ~73,000 years BP, share any similar Pb isotopic ratios with the MDB samples. In contrast, several of the samples from Coats Land analysed by Planchon et al. (2003), which have an age range going back to ~1840 AD, plot close to some of the Australian samples. Finally, 2 samples of snow analysed by Jagoutz et al. (2004) from Berkner Island [see Fig. 2] have compositions that plot away from the Australian array. Another attempt at comparing the EPICA Dome C samples with those from the MDB is to plot the same data set used to prepare Fig. 7, but this time different symbols are used to pin down the age of the EPICA samples which share some similarity with the Australian samples (Fig. 9). Error bars have been omitted for clarity. We also have plotted the MDB Pb isotopic data together with those of 3 dune sites in central and Western Australia (encompassing the Central and Great Sandy Deserts; for locations, see Fig. 2) as well as for EPICA Dome C from Vallelonga et al. (2005). In addition, we are using Pb isotopic ratios obtained for different rock types in Patagonia. The latter values have been obtained from the published literature with the assumption that the regolith above or in the vicinity of those lithologies, that consist mainly of basalts, would have the same Pb isotopic values. Those Patagonian Pb isotopic ratios were recalculated from the ratios presented in tables in those papers and cover 2 different regions, central Argentinian Patagonia and the Patagonian Plateau of southernmost South America. The Pb isotopic ratios data from Argentina are from Stern et al. (1990) for Cenozoic cratonic basalts and transitional basalts [labelled differently in Fig. 10]. The Pb data from the Jurassic Patagonian andesites are also separated into 2 categories in Fig. 10 and these relate to the 2 different groups recognized by Dejonghe et al. (2002).

7.2. Sr and Nd isotopes

As part of the geochemical investigations of the clay fraction of fluvial samples from the MDB, Gingele and De Deckker (2005) examined ^{87}Sr/^{86}Sr and ^{143}Nd/^{144}Nd isotopic ratios using the same

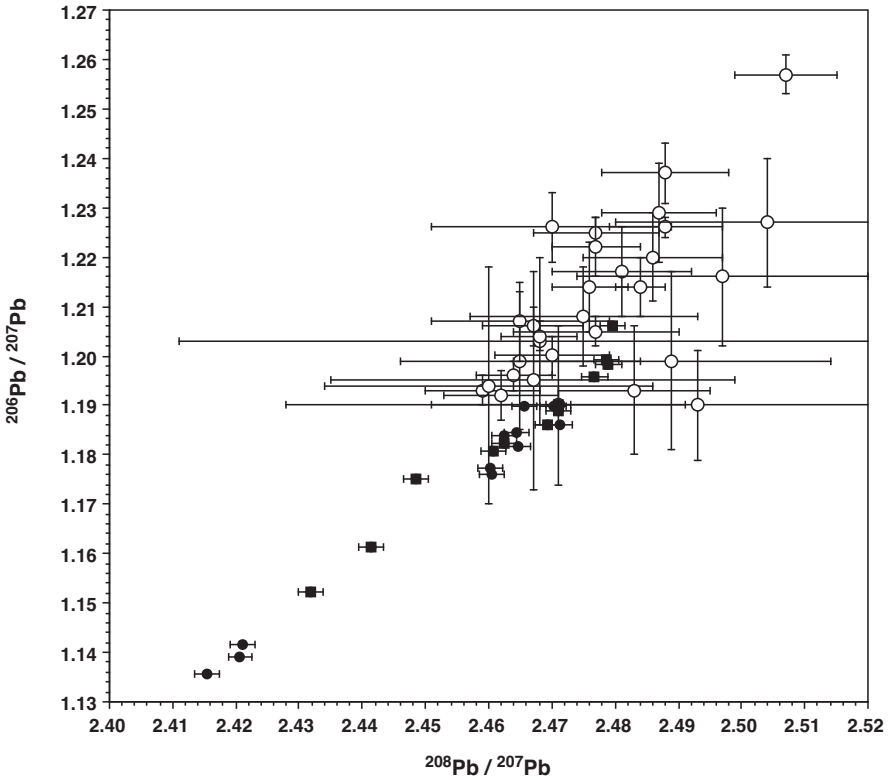

Fig. 7. Plot of the ^{208}Pb/^{207}Pb versus ^{206}Pb/^{207}Pb values obtained from the fluvial clay fraction samples from 23 sites in the Murray Darling Basin [black dots represent Murray-sub-basin samples and black squares Darling sub-basin ones] and the same ratios obtained by Vallelonga et al. (2005) from dust in the Antarctic ice core from EPICA Dome C [open circles]. Note the large error bars for the EPICA samples due to their extremely small sizes.

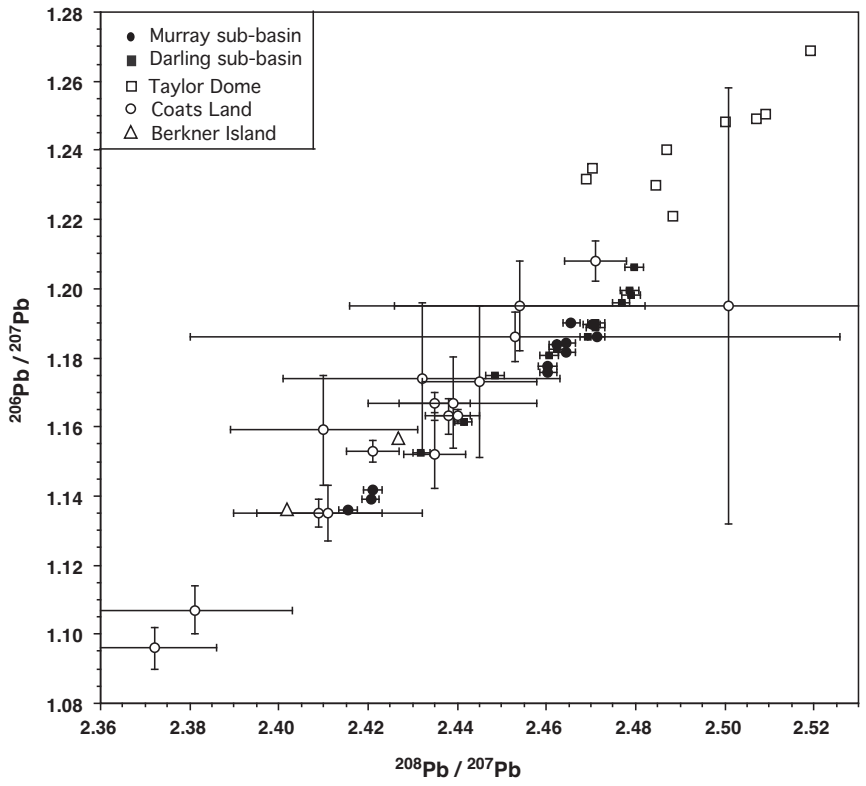

Fig. 8. Plot of $^{208}Pb/^{207}Pb$ versus $^{206}Pb/^{207}Pb$ values obtained from fluvial clay fraction samples from 23 sites in the Murray Darling Basin [black dots represent Murray-sub-basin samples and black squares Darling sub-basin ones] and the same ratios obtained for snow from Coats Land (open circles) by Planchon et al. (2003), spanning an age range of 1990 until ~1840 y AD, and Taylor Dome ice (open square) by Matsumoto and Hinkley (2001), spanning an age range of ~1300 y BP and ~72,900 y BP. Two analyses of snow from Berkner Island (Jagoutz et al., 2004) (open triangles) are also presented for comparison.

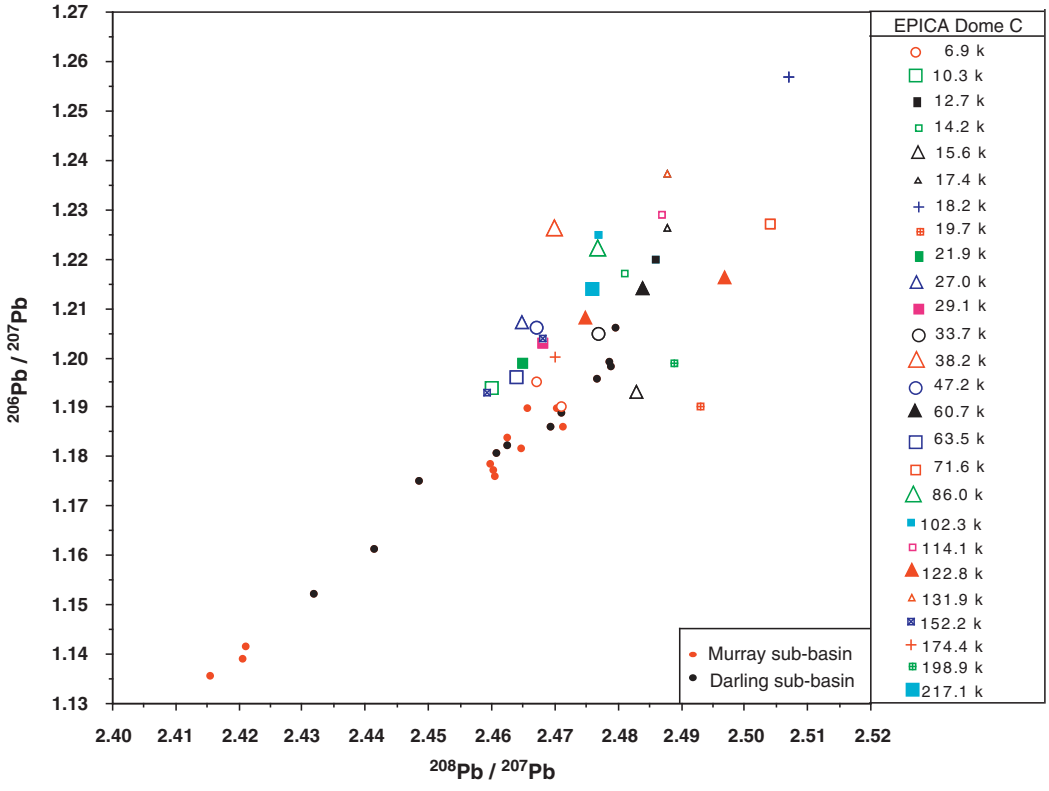

Fig. 9. Plot of the $^{208}Pb/^{207}Pb$ versus $^{206}Pb/^{207}Pb$ values obtained from fluvial clay fraction samples from 23 sites in the Murray Darling Basin [red and black dots] and from dust in the Antarctic ice core from EPICA Dome C by Vallelonga et al. (2005) for different ages which are represented by different symbols in the insert box. See Fig. 7 for error bars.

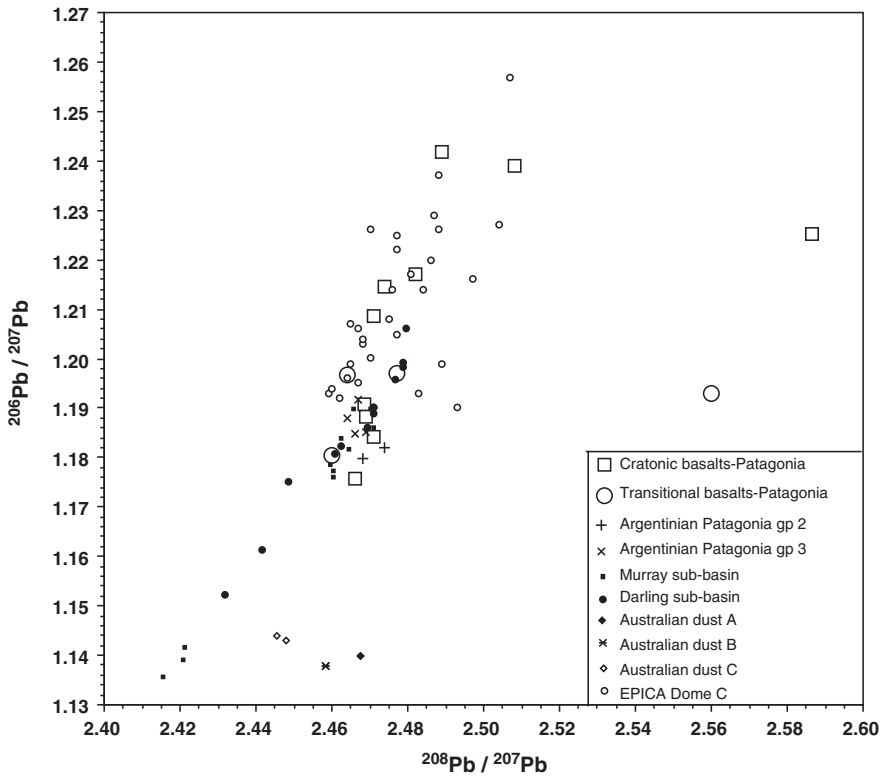

Fig. 10. Plot of $^{208}Pb/^{207}Pb$ versus $^{206}Pb/^{207}Pb$ values obtained from fluvial clay fraction samples from 30 sites in the Murray Darling Basin [black dots represent Murray-sub-basin samples and black squares Darling sub-basin ones] as well as those for 3 dust samples (A–C) from desertic areas of Western Australia [for location refer to Fig. 2] for comparison with the same Pb isotopic rations obtained from different lithologies in Patagonia. The data from Argentina are from Stern et al. (1990) for Cenozoic cratonic basalts [open squares] and transitional basalts (open circles). Data from Jurassic Patagonian andesites are separated into 2 categories which relate to 2 different groups recognized by Dejonghe et al. (2002) and these are represented by (+) and (x).

samples discussed here. We compare these ratios with those of the dust samples recovered from various levels in the ice core taken at EPICA Dome C as well as other locations such as Dome B and Old Dome B, Vostok and Komsomolskaya (Delmonte et al., 2004, 2007, plus *pers. comm*. to De Deckker). Note that 26 samples from the MDB were analysed for Sr and Nd isotopes, instead of 23 for Pb isotopes. Unfortunately, the EPICA Dome C samples analysed by Delmonte and her colleagues [*op. cit.*] do not originate from the same depths for those analysed by Vallelonga et al. (2005), otherwise comparison between the 3 sets of isotopes could have been clearly established. Note that several of the MDB samples plot close to some of the Antarctic samples (Fig. 11), but it is nevertheless obvious that the majority of the Murray sub-basin samples plot away from the ice core samples. The insert in Fig. 11 better defines the various data points of interest to the Antarctic samples.

7.3. HYSPLIT simulations

Six dust events were chosen for simulation: September, October and November 2002, February and December 2005, and April 2008. The HYSPLIT simulations were run for 7–11 days, depending on the size of the archive. The positions of all particles emitted during the simulations were output every 6 h for later plotting. A Fortran program was used to code the particle locations with keyhole markup language (KML) tags for display in Google Earth ™. Concentration calculations were made but not displayed.

Results from the HYSPLIT simulations (see Fig. 4 and Appendices A–E available in colour on the *Palaeo-3* web site) demonstrate the potential for dust transport from Australia to both Antarctica and Patagonia. Some particles from all simulations pass over the Antarctic continent, albeit often up to several kilometers above the surface and after a travel distance of approximately 13,000 km. Mechanisms by which the elevated dust particles may reach the surface remain problematic.

HYSPLIT uses gravitational settling to calculate dry deposition of the dust particles. The high number of particles reaching South America in our initial simulations caused us to question how effective this process was. For PM10, the settling rate as calculated by HYSPLIT was ~7.3E-4 m s^{-1}. Trials using the November 2002 case showed that increasing the settling rate by a factor of 10 actually increased the number of particles reaching Antarctica after 120 h. Maring et al. (2003), studying African dust transport across the Atlantic, 5000 km downwind of the dust source, found that Stokes Law overestimated dust removal by settling. In their investigations, more accurate results were obtained by adding a small upward vector to the gravitational settling velocity. In light of this, it was decided to use the default setting for this study.

8. Discussion

8.1. Pb isotope evidence

It is difficult to argue with great confidence that the MDB is a source of aeolian dust over the last 217 Ka because of the error bars justifiably placed on the EPICA Dome C samples by Vallelonga et al. (2005). Nevertheless, there are several ice-core samples that have $^{208}Pb/^{207}Pb$ and $^{206}Pb/^{207}Pb$ which plot very close to MDB values. In particular, examination of Fig. 9 shows that the dust deposited at Dome C at 6.9 Ka [at least one of the 2 samples], at 33.7 Ka, at 47.2 Ka, and one sample at 122.8 Ka plot close to samples from the MDB. These samples correspond to deposition during interglacial periods [6.9 ka and 122.8 Ka] or during periods [33.7 and 47.2 Ka] when SE Australia was extremely wet, a period which Bowler et al. (2006) refer to as the

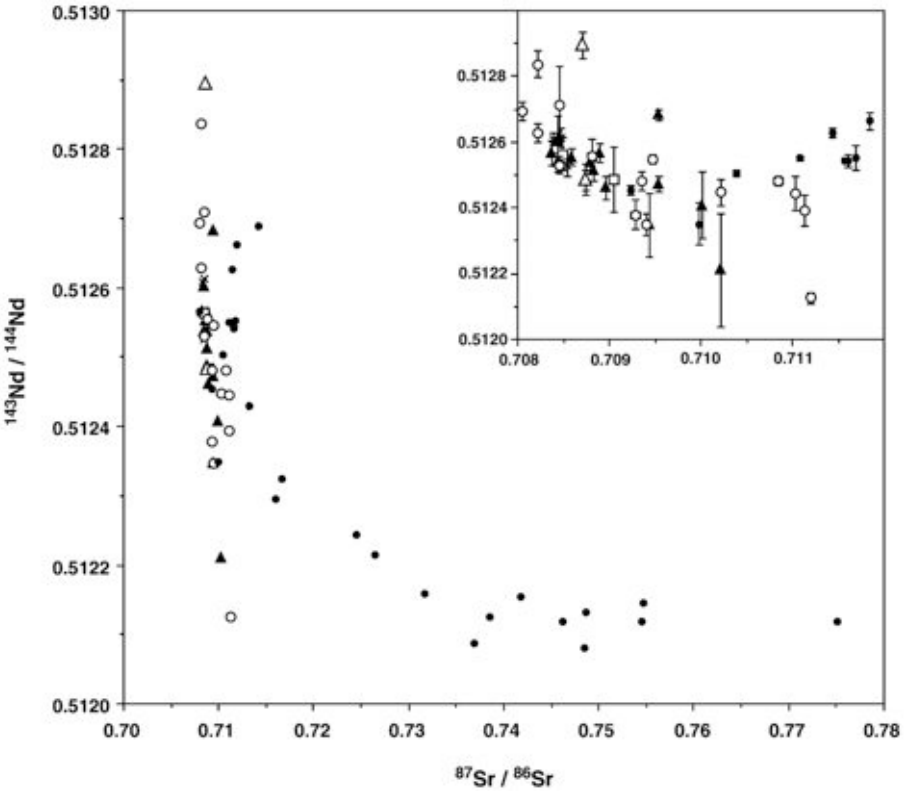

Fig. 11. Plots of $^{87}Sr/^{86}Sr$ versus $^{143}Nd/^{144}Nd$ values obtained from fluvial clay fraction samples from 32 sites in the Murray Darling Basin [black dots; data from Gingele and De Deckker, 2005], and from dust samples from various ice cores. These are: Vostok [open circles], EPICA Dome C [black triangles], Dome B [cross], Old Dome C [open triangles] and Komsomolskaya [open square]. Those data from Antarctica were taken from Delmonte et al. (2004, 2007, plus pers. comm. to De Deckker). The insert shows that some of the Darling sub-basin clays have similar values to some Antarctic samples and that most of the Murray sub-basin samples, and several from the Darling sub-basin, which have $^{87}Sr/^{86}Sr$ values >0.72 are clearly outside the range of values of the Antarctic samples.

'megalake phase' corresponding to Marine Isotope Stage 3 (Fig. 9).This appears to be consistent with an expanded monsoon trough and by a poleward expansion of the Hadley cell bringing dust transport closer to Antarctica. The dust material that would have been deposited during glacial periods [e.g. those from 19.7 and 21.9 Ka] is clearly outside the range of the MDB material and, consequently, would argue for a different source or possibly a mixture of sources. The dust concentration in the ice cores in Antarctica is much higher during glacial periods (Petit et al. (1999), and in particular at Dome C as demonstrated by Vallelonga et al., 2005). Additional information was discussed on major elements in Marino et al. (2008) and on the full cortège of rare earth elements in Gabrieli et al. (in press).

Since access to samples of the Patagonian regolith to analyse Pb isotopes has not yet been possible, we refer to published data on host rocks [Jurassic andesites] from central Argentinian Patagonia (Dejonghe et al., 2002) and Patagonian Plateau basalts [Pliocene to Quaternary in age] (Stern et al., 1990) in order to compare the data with those which Vallelonga et al. (2005) obtained for the EPICA Dome C core. The data are plotted in Fig. 10 together with three additional dust samples from dune fields from Central Australia and northern Western Australia already discussed in Gingele et al. (2007) for which Sr and Nd isotopes analyses were made [refer to sites A–C in Fig. 2]. It is evident that the dust is not derived from the recent weathering of Archean crust, as due to their age, an older decay would plot far away from those values for the regolith resulting from the younger MDB lithologies This implies that there is no evidence for dust from the Australian craton thus far recognized in Antarctic dust samples, a conclusion that is further supported by the atmospheric circulation models [refer to Fig. 4 and Appendices A–E to examine common trajectories].

Patagonian lithologies, on the other hand, have Pb isotopic signatures that have a great degree of similarity with some of the EPICA Dome C samples. Interestingly, several of the Patagonia lithologies plot very close to several MDB samples. This similarity that appears to argue for a Patagonian origin of several Antarctic dust layers will have to be addressed once the regolith [especially fluvial sediments] in this part of South America is systematically analysed for Pb isotopes, in combination with other isotopes and elements [see discussion below]. We argue that care will have to be taken to ensure that some of the dust sampled at the surface of the Patagonian landscape is not contaminated with material or soil possibly originating from Australia! The best way to address this issue is to study several dated profiles and demonstrate the uniformity of the isotopic signatures down the sequence. For example, Mee et al. (2004) showed that Sr isotopes in a soil profile in SE South Australia differ from the Tertiary limestone it overlies, arguing for an aeolian origin for the soil. It is also interesting that the Berkner Island snow samples analysed by Jagoutz et al. (2004) do not have either a Patagonian or Australian Pb isotopic signature (Fig. 8).

8.2. Additional clues obtained from Sr and Nd isotopes

Revel-Rolland et al. (2006) argued for eastern Australia to have been a source of dust in East Antarctica. In particular, they thought that the Lake Eyre region dust signature overlaps with Antarctic dust signatures, and particularly that during interglacial periods (Holocene and Marine Isotopic Stage 5e) Australia would have been a dominant supplier of dust to Antarctica. Our data presented in Fig. 11 and its insert support those findings, but also show that several of the Darling sub-basin signatures plot very close to many of the Antarctic ice core

samples [although the Murray-sub-basin fluvial clays that have a range of $^{143}Nd/^{144}Nd$ values of <0.51235 [or <−6 ε_{Nd} (0)] clearly plot outside the range of Antarctic values. Of interest is that the Darling-sub-basin is geographically located to the east and southeast of Lake Eyre, but both [Eyre and Darling] basins belong to different drainage systems. Unpublished data supplied by Dr B. Delmonte [*pers. com.* to De Deckker] show that Nd and Sr isotopic ratios link Lake Eyre dust with that found at Vostok at 262 Ka and Dome C at stage 20 (~800 Ka).

8.3. Atmospheric circulation in the Southern Hemisphere

Sea-salt Na concentrations in the DSS [Law Dome] ice core, for the past 45,000 years, are currently being analysed, and so far only unpublished coarse data at centennial averages have been completed (Mark Curran, ACE CRC and Australian Antarctic Program, Hobart, Australia, pers. comm. to Goodwin). These data indicate that Na concentrations were lower than the mean value for the past century at 15.6 Ka, 29.1 Ka and 33.7 Ka which is indicative of positive Southern Annular Mode [=+ve SAM] atmospheric circulation, similar to the 1884 to 1908 AD period discussed above. However, during the LGM, around 21.9 Ka, Na concentrations in the DSS core are higher (4 to 5 μeq/L) than the mean for the past century (3.7 μeq/L), and are therefore indicative of pressure and wind anomalies south of Australia that are consistent with a weakened circumpolar trough or poleward subtropical ridge associated with the +ve SAM phase.

This apparent inconsistency in the hypothesized circulation changes responsible for dust transport during the LGM can be explained by the modelling results of Justino and Peltier (2006) (shown in Fig. 5). Their GCM experiment produced a dominant SH climate mode during LGM winter that resembles the negative ENSO/Pacific South American mode (PSA1 −ve or La Nina-like state) of Mo and Higgins (1998), replacing the SAM as the dominant mode of climate variability. This three-wave number mode or wave-train is characterized by high-pressure anomalies south of SE Australia and New Zealand that are typical of high frequency atmospheric blocking, such as occurred during the 1884 to 1908 period, described above in Section 4. The high frequency atmospheric blocking events are synoptic characteristics when the atmospheric circulation is in either the positive SAM or PSA negative phase circulation modes. The associated poleward air trajectories from the south-east of Australia traverse the circumpolar trough and transport aerosols into East and West Antarctica. We therefore argue that it is during periods of significant drought during interglacials, such as conditions currently being experienced in SE Australia and which also occurred between 1895 and 1902 [termed the 'Federation Drought' (see: http://www.bom.gov.au/lam/climate/levelthree/c20thc/drought1.htm)] that aeolian dust can more easily reach parts of Antarctica, as air masses circumnavigate Antarctica, and in the process dust can reach parts of Patagonia as well.

9. Conclusions

We argue here that SE Australia, and in particular the dry Darling sub-basin, as well as central Australia [viz. the Lake Eyre region] are a source of airborne dust to parts of Antarctica as well as to Patagonia. This dust pathway appears to be activated by changes in Southern Hemisphere circulation, namely a poleward migration of the subtropical ridge and the westerlies, together with an increased frequency of blocking high pressure systems. It is during interglacials, such as today, and in particular during periods of intensive drought, that airborne dust can reach Antarctica, especially its coastal fringes. To test this hypothesis, it would be worthwhile to conduct a coring campaign in the Pacific sector of the Southern Ocean which, following our atmospheric observations [see Fig. 4 and Appendices A–E] and modelling, show a vast quantity of dust in transit over that part of the ocean today. Equally some ice cores from East Antarctica, near the Ross Sea for example, would test our hypothesis.

De Deckker et al. (2008) showed that a cortège of insoluble lanthanides [e.g. Praesodymium [Pr], Samarium [Sm], Gadolinium [Gd] and Dysprosium [Dy]] analysed on the MDB samples can help to 'fingerprint' clay-fraction material and thus identify its origin. If that were applied to ice core samples, in addition to Nd, Pb and Sr isotopes on the same samples, it may be possible, once and for all, to identify the source or sources of dust in Antarctic ice cores.

Dust traps should also be placed in Patagonia to identify the material that falls there and also monitor atmospheric circulation and air masses prior to and at the time of dust fall out.

We now have data that support Joussaume's (1993) models and which can help argue for a source of Australian dust in Antarctica. Already, her work has been endorsed by the recent findings of Li et al. (2008) who argue for Australian mineral dust supply to the Pacific sector of the Southern Ocean, and we would argue that some of that dust can reach the southern tip of South America as well Antarctica.

Acknowledgements

Funding for the Pb isotopes was provided to PDD by a grant from the Murray Darling Basin Commission. Some aspects of the research were also supported by ARC Discovery grant 0772180 awarded to PDD and colleagues. PDD is also grateful to Dr B. Delmonte who provided unpublished data and for numerous discussions at an early stage of the manuscript preparation. Mrs J. Shelley also provided much help with referencing and also commenting on the manuscripts during its many stages. Goodwin's work on Antarctic ice cores is collaborative with Drs T. Van Ommen and M. Curran at the Australian Antarctic Division, and is partly supported by an Australian Antarctic Science (AAS) grant. Goodwin is grateful to Dr M. Curran for personal communication of preliminary sea-salt sodium concentrations from the Law Dome ice core during late Stage 3 and Stage 2 layers.

We are very grateful to Dr M. Reheis for her excellent editorial work and suggestions that significantly improved the quality of the paper, and we thank also Dr J-B. Stuut and Professor T. Corrège for their pertinent review of the paper.

Appendix A

Fig. A. The simulation was commenced on September 15, 2002. A: September 17, after 48 h showing the rapid transport of dust to the southeast of Australia and the plume extends well over ~2500 km past New Zealand; B: September 18, after 72 h. Note the clear bifurcation of the plume with some particles being carried eastwards towards the Antarctic continent; C: September 19 after 96 h; D: September 20 after 144 h when some dust particles travelled over Adélie Land and along a line roughly parallel to the Trans-Antarctic Mountains. In addition, some particles travelled over South America; E: 21 September, after 192 h which shows a large concentration of particles over Patagonia, and some over the Weddell Sea and west of the tip of South America. Note that the model simulation for the period of September 15–21, 2002 is characterized by the rapid transport of particles across New Zealand. At 0000 UTC on September 16, the southern-most particles were south of Tasmania. Over the next 24 h, the particles averaged over 140 km h^{-1} to arrive in the position shown in A.

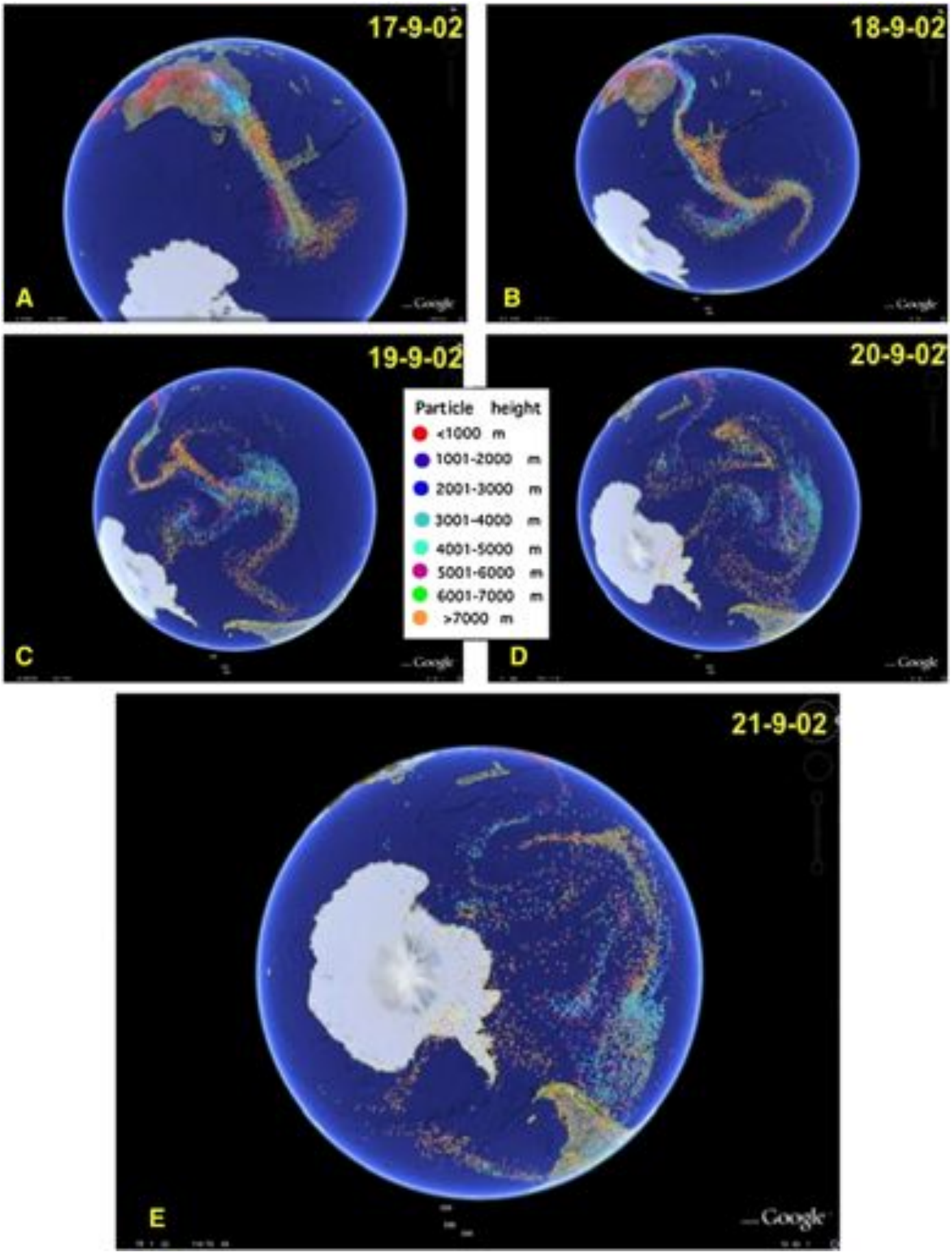
17-9-02
A
18-9-02
B
19-9-02
C
Particle height
<1000 m
1001-2000 m
2001-3000 m
3001-4000 m
4001-5000 m
5001-6000 m
6001-7000 m
>7000 m
20-9-02
D
21-9-02
E
Google

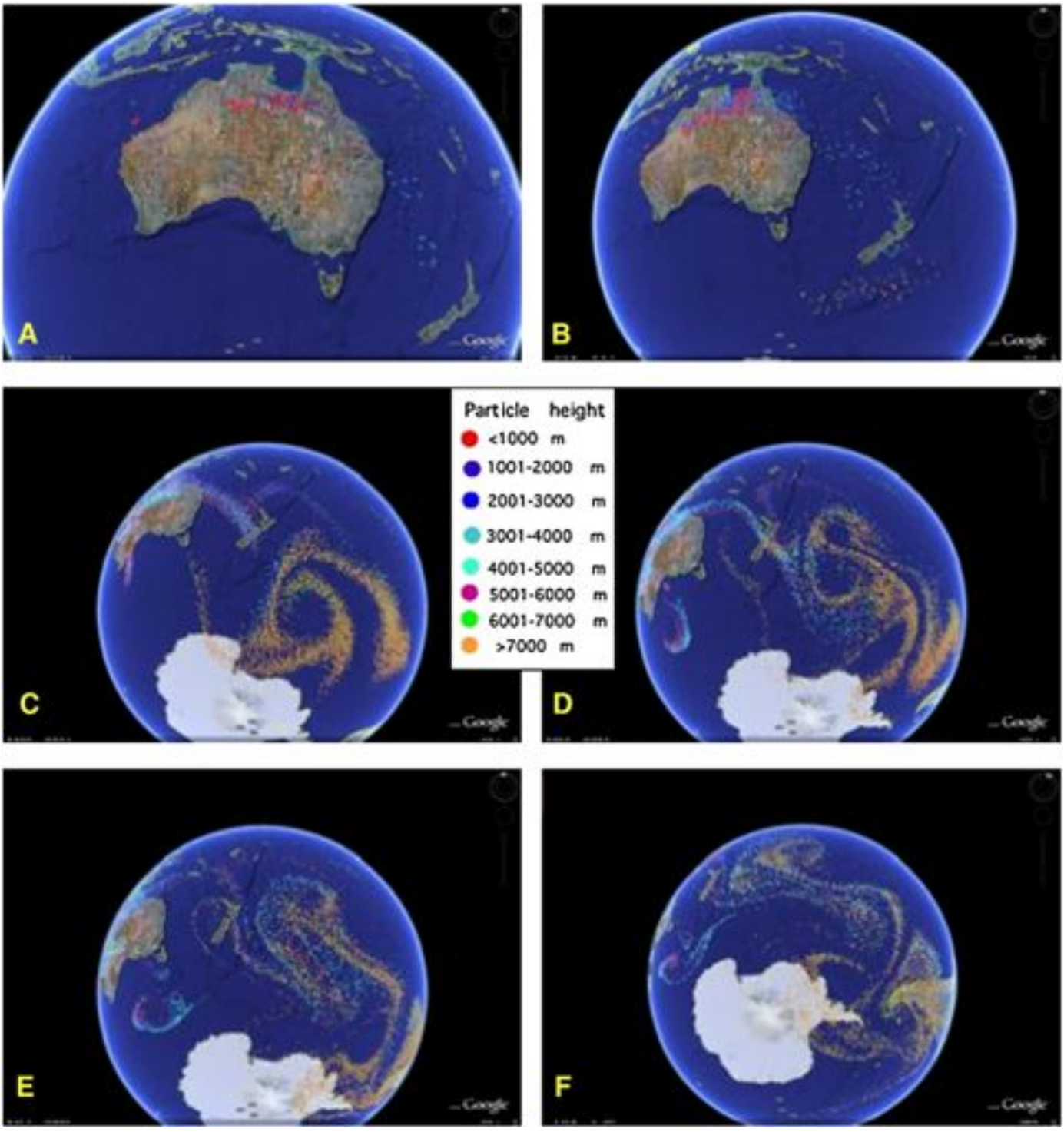

Fig. B. The simulation was commenced on October 21, 2002 at 0000 UTC. A: October 23, after 72 h. Yellow dots show sources used in all simulations, but a concentration of particles at low altitude occurs in the central northern part of Australia; B: October 24, after 96 h when many particles will have passed over New Zealand; C: October 27, after 144 h. Large number of particles in the Ross Sea associated with a spectacular gyral system; D: October 28, after 168 h; E: October 29, 2002 after 192 h. Particles over West Antarctica, the Weddell Sea and Patagonia; F: October 30, after 216 h.

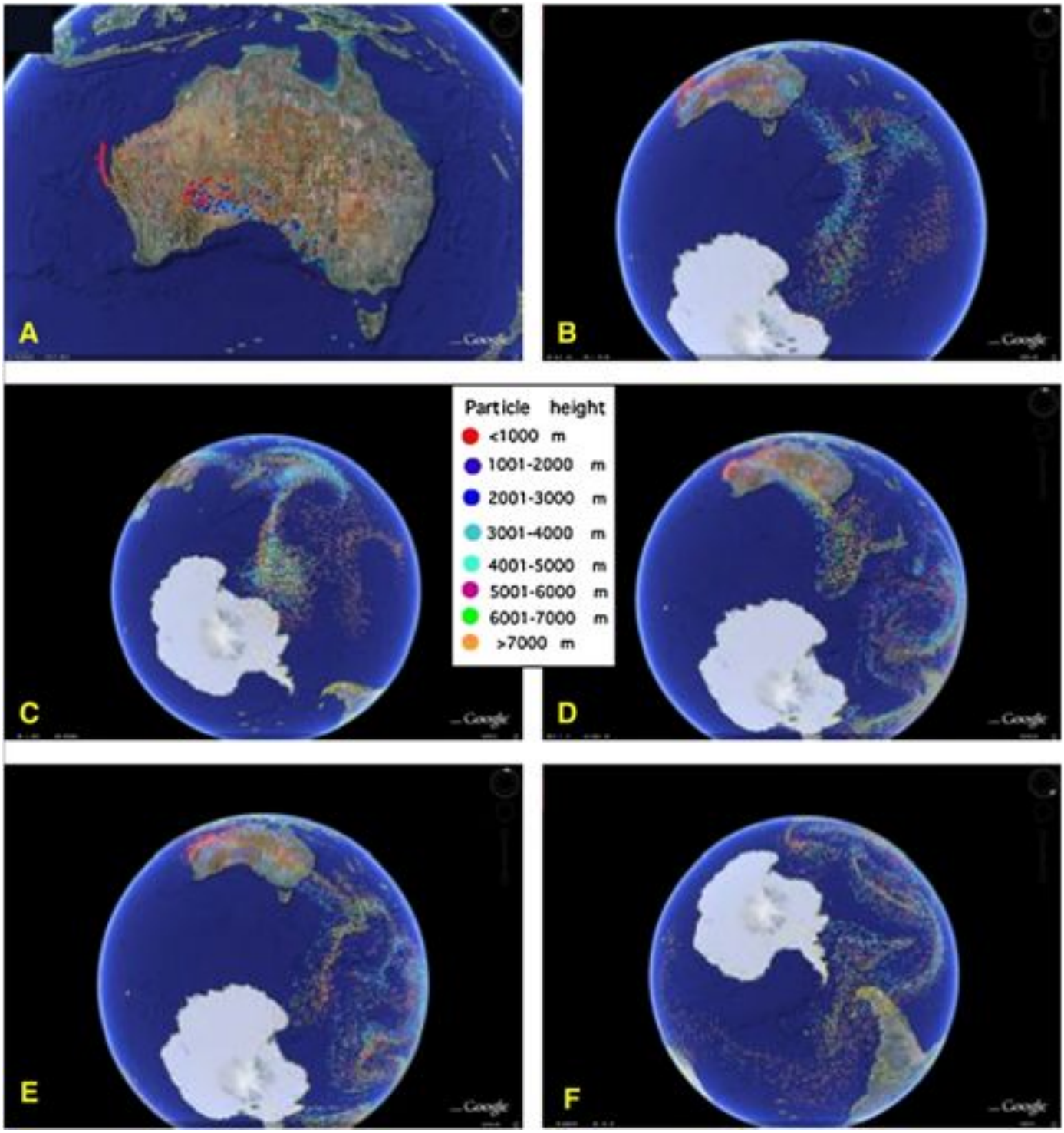

Fig. C. The simulation was commenced on November 10, 2002 at 0000 UTC. A: November 12, after 48 h showing the location of dust entrainment (yellow dots) and the dust being lifted in Western Australia, including offshore; B: November 14, after 96 h showing the passage of dust particles over the Tasman Sea and down towards the Ross Sea. Note also the pathway of particles at <1000 m offshore NW Eastern Australia, thus showing that 2 dust plumes co-existed in opposite directions; C: November 15, after 120 h with the large concentration of dust particles in the Southern Ocean opposite the Ross Sea; D: November 17, after 168 h when a second plume of dust particles travelled over the Tasman Sea and East Antarctica and the Ross Sea dust concentration from the previous simulation now having progressed towards the Transantarctic Mountains and Patagonia; E: November 18, after 192 h showing the trajectory of the dust plume over Drakes Passage and into the southern Atlantic ocean as is visible in F on November 19, after 216 h.

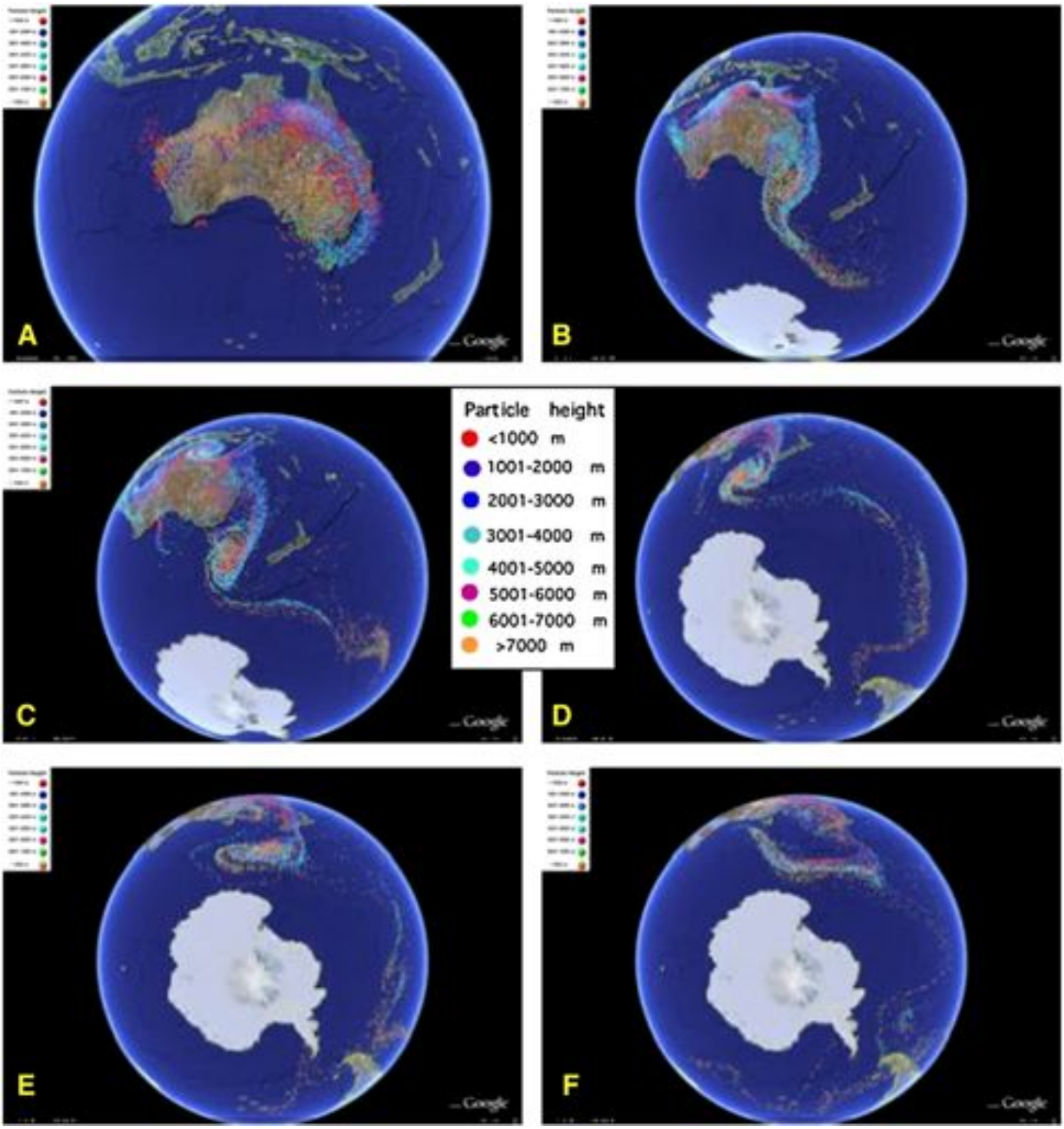

Fig. D. The simulation was commenced on February 1, 2005 at 0000 UTC. A: February 2 after 48 h showing a large number of particles transient over the eastern and northwestern coasts of Australia; B: February 4 after 96 h when the eastern Australian plume of dust particles has travelled over Tasmania and the southern portion of the Tasman Sea, whereas at low latitudes several plumes are bordering the northern and northwestern coasts of Australia; C: February 5 after 96 h. Note the 3 cyclonic circulations over Australia, Cyclone Harvey [3–7 February 2005] over the Gulf of Carpentaria, Cyclone Vivienne [4–9 February 2005] off the northwest WA coast and the Low south of Tasmania [which produced some huge downpours of rain in Victoria]; D: February 7 after 144 h showing that the dust particles are located far away from Antarctica, although some are reaching the tip of Patagonia; E: February 8 after 168 h when the breaking up of the plumes has dispersed the dust particles close to the Ross sea and west of the South American Peninsula; F: February 8 after 192 h with many particles over the tip of Patagonia and on either side of it.

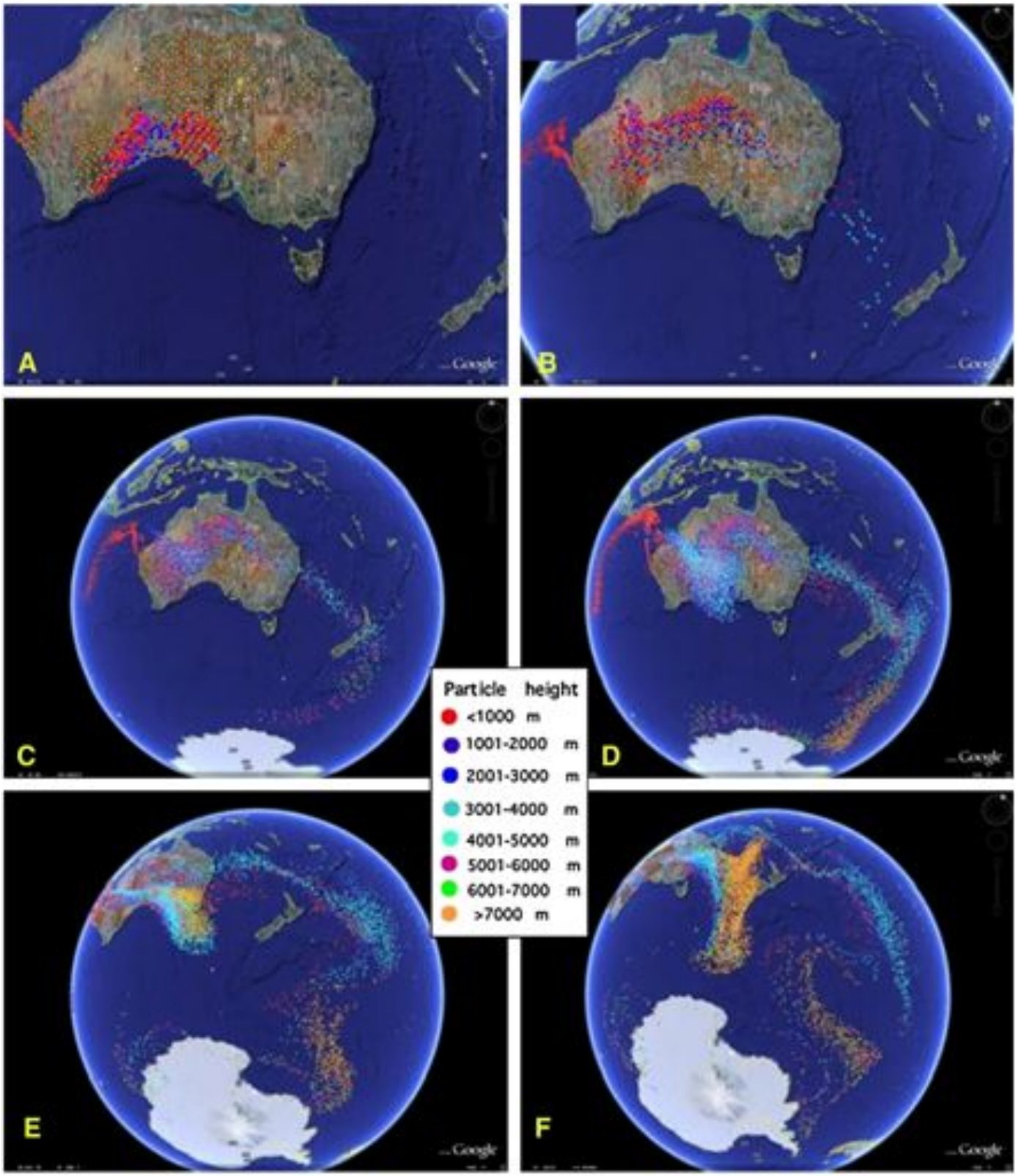

Fig. E. The simulation was commenced on 22 December, 2005 at 1200 UTC. A: December 23, 2002 after 24 h when dust particles at low altitude concentrate over a large part of central and western Australia; B: December 24, 2002 after 48 h when the dust entrainment has forced the dust plumes to expand towards and over part of the Tasman Sea and the eastern Indian Ocean; C: December 26, 2002 after 72 h shows the spectacular positioning of dust particles in the central part of the Indian Ocean, as well as east of New Zealand, with a continuation towards the Ross Sea, and also material along the Antarctic coast as far as Adélie Land; D: December 27, 2002 after 96 h. Note the eastward-moving particles along the coast of East Antarctica and also in the western part of the Pacific Ocean; E: December 28, 2002 after 120 h; F: December 29, 2002 after 144 h, by then the dust plume has increased in altitude over the New Zealand region.

References

Barrows, T.T., Juggins, S., De Deckker, P., Thiede, J., Martinez, J.I., 2000. Sea-surface temperatures of southwest Pacific Ocean during the Last Glacial Maximum. Paleoceanography 15, 95–109.

Basile, I., Grousset, F.E., Revel, M., Petit, J.R., Biscaye, P.E., Barkov, N.I., 1997. Patagonian origin of glacial dust deposited in East Antarctica (Vostok and Dome C) during glacial stages 2, 4 and 6. Earth and Planetary Science Letters 146, 573–589.

Bowler, J.M., 1976. Aridity in Australia: age, origins and expressions in aeolian landforms and sediments. Earth Science Reviews 12, 279–310.

Bowler, J.M., 1981. Australian salt lakes: a palaeohydrologic approach. Hydrobiologia 82, 431–444.

Bowler, J.W., Kotsonis, A., Lawrence, C.R., 2006. Environmental evolution of the Mallee region, Western Murray Basin. Proceedings of the Royal Society of Victoria 118 (2), 161–210.

Butler, B.E., Hubble, G.D., 1978. The general distribution and character of soils in the Murray–Darling River system. Proceedings of the Royal Society of Victoria 90, 149–156.

Calvo, E., Pelejero, C., De Deckker, P., Logan, G.A., 2007. Antarctic deglacial pattern in a 30 kyr record of sea surface temperature offshore South Australia. Geophysical Research Letters 34, L13707. doi:10.1029/2007GL029937.

Chan, Y.-C., McTainsh, G., Leys, J., McGowan, H., Tews, K., 2005. Influence of the 23 October 2002 dust storm on the air quality of four Australian cities. Water, Air, and Soil Pollution 164, 329–348.

Chen, J.H., Wasserburg, G.J., 1981. Isotopic determination of uranium in picomole and sub-picomole quantities. Analytical Chemistry 53, 2060–2067.

Chow, T.J., Patterson, C.C., 1962. The occurrence and significance of lead isotopes in pelagic sediments. Geochimica et Cosmochimica Acta 26, 263–308.

Close, A., 1990. The impact of man on the natural flow regime. In: Mackay, N., Eastburn, D. (Eds.), The Murray. Murray Darling Basin Commission, Canberra, Australia, pp. 61–74.

De Deckker, P., 1982. Holocene history of four maar lakes in SE Australia, illustrated by the recovery of ostracods and other invertebrate and fish remains. Proceedings of the Royal Society of Victoria 94, 183–220.

De Deckker, P., Abed, R.M.M., de Beer, D., Hinrichs, K., O'Loingsigh, T., Schefuß, E., Stuut, J.-B., Tapper, N.J., van der Kaars, S., 2008. Geochemical and microbiological fingerprinting of airborne dust that fell in Canberra, Australia, in October 2002. Geochemistry Geophysics Geosystems 9, Q12Q10. doi:10.1029/2008GC002091.

Dejonghe, L., Darras, B., Hughes, G., Muchez, P., Scoates, J.S., Weis, D., 2002. Isotopic and fluid-inclusion constraints on the formation of polymetallic vein deposits in the central Argentinian Patagonia. Mineralium Deposita 37, 158–172.

Delmonte, B., Anderson, P.S., Hanson, M., Schönberg, H., Petit, J.R., Basiel-Doelsch, I., Maggi, V., 2008. Aeolian dust in East Antarctica (EPICA-Dome C and Vostok): provenance during glacial ages over the last 800 kyr. Geophysical Research Letters 35, LO7703. doi:10.1029/2008GL033382.

Delmonte, B., Basile-Doelsch, I., Petit, J.R., Maggi, V., Revel-Rolland, M., Michard, A., Jagoutz, E., Grousset, F., 2004. Comparing the Epica and Vostok dust records during the last 220,000 years: stratigraphical correlation and provenance in glacial periods. Earth Science Reviews 66, 63–87.

Delmonte, B., Petit, J.R., Basile-Doelsch, I., Jagoutz, E., Maggi, V., 2007. Late Quaternary Interglacials in East Antarctica from ice core dust records. In: Sirocko, F., et al. (Ed.), The Climate of Past Interglacials. Developments in Quaternary Science, vol. 7. Elsevier, New York, pp. 53–73.

Douglas, G.B., Gray, C.M., Hart, B.T., Beckett, R., 1995. A strontium isotopic investigation of the origin of suspended matter (SPM) in the Murray–Darling River system. Geochimica et Cosmochimica Acta 59, 3799–3815.

Draxler, R.R., Gillette, D.A., Kirkpatrick, J.S., Heller, J., 2001. Estimating PM_{10} air concentrations from dust storms in Iraq, Kuwait, and Saudi Arabia. Atmospheric Environment 35, 4315–4330.

Draxler, R.R., Hess, G.D., 1998. An overview of the Hysplit-4 modelling system for trajectories dispersion and deposition. Australian Meteorological Magazine 47, 295–308.

Frank, M., 2002. Radiogenic isotopes: tracers of past oceanic circulation and erosional input. Reviews of Geophysics 40, 1–38.

Gabrieli, P., Wegner, A., Petit, J.R., Delmonte, B., De Deckker, P., Gaspari, V., Fisher, H., Ruth, U., Kriews, M., Boutron, C., Cescon, P., Barbane, C. in press. A major glacial interglacial change in aeolian dust composition as inferred from Rare Earth Elements in Antarctic ice. Quaternary Science Reviews. doi:1016/j.quascirev.2009.09.002.

Gagan, M.K., Ayliffe, L.K., Beck, J.W., Cole, J.E., Druffel, E.R.M., Dunbar, R.B., Schrag, D.P., 2000. New views of tropical paleoclimates from corals. Quaternary Science Reviews 19, 45–64.

Gaiero, D.M., 2007. Dust provenance in Antarctic ice during glacial periods: from where in southern South America? Geophysical Research Letters 34, L17707. doi:10.1029/2007GL030520.

Gaudichet, A., Angelis, M.D., Lefevre, R., Petit, J.R., Korotkevitch, Y.S., Petrov, V.N., 1988. Mineralogy of insoluble particles in the Vostok Antarctic ice core over the last climatic cycle (150 Kyr). Geophysical Research Letters 15, 1471–1474.

Gingele, F.X., De Deckker, P., 2004. Fingerprinting Australia's rivers with clay minerals and the application for the marine record of climate change. Australian Journal of Earth Sciences 51, 339–348.

Gingele, F.X., De Deckker, P., 2005. Clay mineral, geochemical and Sr–Nd isotopic fingerprinting of sediments in the Murray–Darling fluvial system, southeast Australia. Australian Journal of Earth Sciences 52, 965–974.

Gingele, F.X., De Deckker, P., Norman, M., 2007. Late Pleistocene and Holocene climate of SE Australia reconstructed from dust and river loads deposited offshore the River Murray Mouth. Earth and Planetary Science Letters 255, 257–272.

Goodwin, I., de Angelis, M., Pook, M., Young, N.W., 2003. Snow accumulation variability in Wilkes Land, East Antarctica and the relationship to atmospheric ridging in the 130° to 170° E region since 1930. Journal of Geophysical Research 108 (D21), 4673. doi:10.1029/2002JD002995.

Goodwin, I.D., van Ommen, T.D., Curran, M.A.J., Mayewski, P.A., 2004. Mid latitude winter climate variability in the south Indian and south-west Pacific regions since 1300 AD. Climate Dynamics 22, 783–794. doi:10.1007/S00382-004-0403-3.

Grousset, F.E., Biscaye, P.E., 2005. Tracing dust sources and transport patterns using Sr, Nd, and Pb isotopes. Chemical Geology 222, 149–167.

Grousset, F.E., Biscaye, P.E., Revel, M., Petit, J.R., Pye, K., Joussaume, S., Jouzel, J., 1992. Antarctic (Dome C) ice-core dust at 18 k.y. BP. Isotopic constraints on origins. Earth and Planetary Science Letters 111, 175–182.

Gulson, B.L., 1986. Lead isotopes in Mineral Exploration. Elsevier, Amsterdam. 245 pp.

Jagoutz, E., Bory, A., Jotter, R., Zartman, R., 2004. Pb, Nd and Sr isotopes in aerosols extracted from snow, Berkner Island, Antarctica. Lunar and Planetary Science 35 abstract #1530.

Jennings, J., 1968. A revised map of the desert dunes of Australia. Australian Geographer 10, 408–409.

Joussaume, S., 1993. Paleoclimatic tracers: an investigation using and atmospheric general circulation model under ice age conditions 1. Desert dust. Journal of Geophysical Research 98 (D2), 2767–2805.

Justino, F., Peltier, W.R., 2006. Influence of present day and glacial surface conditions on the Antarctic Oscillation/Southern Annular Mode. Geophysical Research Letters 33, L22702. doi:10.1029/2006GL027001.

King, J.C., Turner, J., 1997. Antarctic Meteorology and Climatology. Cambridge University Press, Cambridge.

Li, F., Ginoux, P., Ramaswany, V., 2008. Distributions, transport, and deposition of mineral dust in the Southern Ocean and Antarctica: contribution of major sources. Journal of Geophysical Research 113, D10207. doi:10.1029/2007DJ009190.

Lunt, D.J., Valdes, P.J., 2002. Dust deposition and provenance at the Last Glacial Maximum and present day. Geophysical Research Letters 29 (2), 2085. doi:10.1029/2002GL015656.

Maring, H., Savoie, D.L., Izaguirre, M.A., Custals, L., 2003. Mineral dust aerosol size distribution change during atmospheric transport. Journal of Geophysical Research 108 (D19), 8592. doi:10.1029/2002JD002536.

Marino, F., Castellano, E., Ceccato, D., De Deckker, P., Delmonte, B., Ghermandi, G., Maggi, V., Petit, J.R., Revel-Rolland, M., Udisti, R., 2008. Defining the geochemical composition of the EPICA Dome C ice core dust during the last Glacial–Interglacial cycle. Geochemistry Geophysics Geosystems 9, Q10018. doi:10.1029/2008GC002023.

Matsumoto, A., Hinkley, T.K., 2001. Trace metal suites in Antarctic pre-industrial ice are consistent with emissions from quiescent degassing of volcanoes worldwide. Earth and Planetary Science Letters 186, 33–43.

McLennan, S.M., Hemming, S.R., McDaniel, D.K., Hanson, G.L., 1993. Geochemical approaches to sedimentation, provenance, and tectonics. In: Processes Controlling the Composition of Clastic Sediments (M.J. Johnsson and A. Basu, eds.). Geological Society of America. Special Paper 284, 21–40.

McTainsh, G.H., Burgess, R., Pitblado, J.R., 1989. Aridity, drought and dust storms in Australia (1960–84). Journal of Arid Environments 16, 11–22.

McTainsh, G.H., Chan, Y., McGowan, H., Leys, J., Tews, K., 2005. The 23rd October 2002 dust storm in eastern Australia: characteristics and meteorological conditions. Atmosphere and Environment 2005, 1227–1236.

Mee, A.C., Bestland, E.A., Spooner, N.A., 2004. Age and origin of Terra Rossa soils in the Coonawarra area of South Australia. Geomorphology 58, 1–25.

Miller, G.H., Magee, J.W., Jull, A.J.T., 1997. Low-latitude glacial cooling in the Southern Hemisphere from amino acids in emu eggshells. Nature 385, 241–244.

Mo, K.C., Higgins, R.W., 1998. The Pacific–South American modes and tropical convection during the Southern Hemisphere winter. Monthly Weather Review 126, 1581–1596.

Moros, M., De Deckker, P., Jansen, E., Richard, J., Telford, R.J., 2009. Holocene climate variability in the Southern Ocean recorded in marine sediments off South Australia. Quaternary Science Reviews 28, 1932–1940.

Petit, J.R., Jouzel, J., Raynaud, D., Barkov, N.I., Barnola, J.-M., Basile, I., Bender, M., Chappellaz, J., Davis, M., Delaygue, G., Delmotte, V.M., Kotlyakov, M., Legrand, M., Lipenkov, V.Y., Lorius, C., Pépin, L., Ritz, C., Saltzman, E., Stievenard, M., 1999. Climate and atmospheric history of the past 420,000 years from the Vostok ice core, Antarctica. Nature 399, 429–436.

Planchon, F.A.M., van de Velde, K., Rosman, K.J.R., Wolff, E.W., Ferrari, C.P., Boutron, C.F., 2003. One hundred fifty-year record of lead isotopes in Antarctic snow from Coats Land. Geochimica et Cosmochimica Acta 67, 693–708.

Renwick, J.A., Revell, M.J., 1999. Blocking over the South Pacific and Rossby wave propagation. Monthly Weather Review 127, 2233–2247.

Revel-Rolland, M., De Deckker, P., Delmonte, B., Hesse, P.P., Magee, J.W., Basile-Doelsch, I., Grousset, F., Bosch, D., 2006. Eastern Australia: a possible source of dust in East Antarctica Interglacial ice. Earth and Planetary Science Letters 249, 1–13.

Rogers, J.C., van Loon, H., 1982. Spatial variability of sea level pressure and 500 mb height anomalies over the Southern Hemisphere. Monthly Weather Review 110, 1375–1392.

Rutland, R.W.R., 1976. Orogenic evolution of Australia. Earth Science Reviews 12, 161–196.

Simmonds, I., Keay, K., 2000. Mean Southern Hemisphere extratropical cyclone behavior in the 40-year NCEP–NCAR reanalysis. Journal of Climate 13, 873–885.

Sinclair, M.R., Renwick, J.A., Kidson, J.W., 1997. Low-frequency variability of Southern Hemisphere sea level pressure and weather system activity. Monthly Weather Review 125, 2531–2543.

Stanley, S., De Deckker, P., 2002. A Holocene record of allochthonous mineral grains into an Australian alpine lake; implications for the history of climate change in southeast Australia. Journal of Paleolimnology 27, 207–219.

Stern, C.R., Frey, F.A., Futa, K., Zartman, R.E., Peng, Z., Kyser, T.K., 1990. Trace-element and Sr, Nd, Pb, and O isotopic composition of Pliocene and Quaternary alkali basalts of the Patagonian Plateau lavas of southernmost South America. Contributions to Mineralogy and Petrology 104, 294–308.

Sturman, A.P., Tapper, N.J., 2006. Weather and Climate of Australia and New Zealand 2nd edition. Oxford University Press, Melbourne.

Thompson, D.W.J., Solomon, S., 2002. Interpretation of recent Southern Hemisphere climate change. Science 296, 895–899.

Toggweiler, J.R., Russell, J., 2008. Ocean circulation in a warming climate. Nature 45, 286–288.

Vallelonga, P., van de Velde, K., Candelone, J.-P., Ly, C., Rosman, K.J.R., Boutron, C.F., Morgan, V.I., Mackey, D.J., 2002a. Recent advances in measurement of Pb isotopes in polar ice and snow at sub-picogram per gram concentrations using thermal ionisation mass spectrometry. Analytica Chimica Acta 453, 1–12.

Vallelonga, P., van de Velde, K., Candelone, J.-P., Morgan, V.I., Boutron, C.F., Rosman, K.J.R., 2002b. The lead pollution history of Law Dome, Antarctica, from isotopic measurements on ice cores: 1500 AD to 1989 AD. Earth and Planetary Science Letters 204, 291–306.

Vallelonga, P., Gabrielli, P., Rosman, K.J.R., Barbante, C., Boutron, C.F., 2005. A 220 kyr record of Pb isotopes at Dome C Antarctica from analyses of the EPICA ice core. Geophysical Research Letters 32, L01706. doi:10.1029/2004GL021449.

Wain, A.G., Lee, S., Mills, G.A., Hess, G.D., Cope, M.E., Tindale, N., 2006. Meteorological overview and verification of HYSPLIT and AAQFS dust forecasts for the duststorm of 22–24 October 2002. Australian Meteorological Magazine 55, 35–46.

White, W.M., Albarède, F.A., Telouk, P., 2000. High-precision analysis of Pb isotope ratios by multi-collector ICP-MS. Chemical Geology 167, 257–270.

Winter, B.L., Johnson, C.M., Clark, D.L., 1997. Strontium, neodymium, and lead isotope variations of authigenic and silicate sediment components from the Late Cenozoic Arctic Ocean: implications for sediment provenance and the source of trace metals in seawater. Geochimica et Cosmochimica Acta 61, 4181–4200.

Woodhead, J.D., Volker, F., McCulloch, M.T., 1995. Routine lead isotope determinations using a ^{207}Pb–^{204}Pb double spike: a long-term assessment of analytical precision and accuracy. The Analyst 120, 35–39.